The Company of
Biologists

RESEARCH ARTICLE

Thyroid follicle development requires Smad1/5- and endothelial cell-dependent basement membrane assembly

Mylah Villacorte[1,*], Anne-Sophie Delmarcelle[1,*], Manon Lernoux[1], Mahé Bouquet[1], Pascale Lemoine[1], Jennifer Bolsée[1], Lieve Umans[2,3], Susana Chuva de Sousa Lopes[4], Patrick Van Der Smissen[1], Takako Sasaki[5], Guido Bommer[1], Patrick Henriet[1], Samuel Refetoff[6], Frédéric P. Lemaigre[1], An Zwijsen[2,7], Pierre J. Courtoy[1] and Christophe E. Pierreux[1,‡]

ABSTRACT

Thyroid follicles, the functional units of the thyroid gland, are delineated by a monolayer of thyrocytes resting on a continuous basement membrane. The developmental mechanisms of folliculogenesis, whereby follicles are formed by the reorganization of a non-structured mass of non-polarized epithelial cells, are largely unknown. Here we show that assembly of the epithelial basement membrane is crucial for folliculogenesis and is controlled by endothelial cell invasion and by BMP-Smad signaling in thyrocytes. Thyroid-specific *Smad1* and *Smad5* double-knockout (*Smad1/5*[dKO]) mice displayed growth retardation, hypothyroidism and defective follicular architecture. In *Smad1/5*[dKO] embryonic thyroids, epithelial cells remained associated in large clusters and formed small follicles. Although similar follicular defects are found in *Vegfa* knockout (*Vegfa*[KO]) thyroids, *Smad1/5*[dKO] thyroids had normal endothelial cell density yet impaired endothelial differentiation. Interestingly, both *Vegfa*[KO] and *Smad1/5*[dKO] thyroids displayed impaired basement membrane assembly. Furthermore, conditioned medium (CM) from embryonic endothelial progenitor cells (eEPCs) rescued the folliculogenesis defects of both *Smad1/5*[dKO] and *Vegfa*[KO] thyroids. Laminin α1, β1 and γ1, abundantly released by eEPCs into CM, were crucial for folliculogenesis. Thus, epithelial Smad signaling and endothelial cell invasion promote folliculogenesis via assembly of the basement membrane.

KEY WORDS: Thyroid, Smad1, Smad5, Follicle, Epithelium, Extracellular matrix, Mouse

INTRODUCTION

Thyroid follicles are the functional units of the thyroid gland. Each follicle is composed of a polarized monolayer of epithelial cells delineating a lumen where thyroglobulin (Tg) is stored as colloid. Thyrocytes differentiate from thyroid progenitors that bud from the foregut endoderm as a mass of non-polarized epithelial cells, which reorganize to form prefollicular structures by acquisition of

[1]de Duve Institute and Université Catholique de Louvain, 1200 Brussels, Belgium. [2]VIB Center for the Biology of Disease, KU Leuven, 3000 Leuven, Belgium. [3]Laboratory of Molecular Biology (Celgen), Stem Cell Biology and Embryology, KU Leuven, 2333 Leuven, Belgium. [4]Department of Anatomy and Embryology, Leiden University Medical Center, Leiden, The Netherlands. [5]Department of Matrix Medicine, Faculty of Medicine, Oita University, 879-5593 Oita, Japan. [6]Department of Medicine, Pediatrics and Genetics, The University of Chicago, Chicago, IL 60637, USA. [7]Department of Human Genetics, KU Leuven, Leuven, Belgium.
*These authors contributed equally to this work

‡Author for correspondence (christophe.pierreux@uclouvain.be)

C.E.P., 0000-0002-9647-2816

apicobasal polarity (Fagman et al., 2006; Hick et al., 2013). Differentiated thyrocytes face the lumen at the apical pole, and are attached to the basement membrane at their basal pole. In the mature thyroid, a dense network of blood vessels surrounds each follicle. Together, they form angiofollicular units responsible for T_3 and T_4 thyroid hormone synthesis and storage within luminal Tg, and then hormone secretion into the bloodstream (Colin et al., 2013; Nilsson and Fagman, 2013). A limited number of transcription factors (Nkx2.1, Pax8, Foxe1 and Hhex) and signaling molecules are known to control thyroid development (Fagman and Nilsson, 2010), but the molecular and subcellular morphogenetic machineries regulating follicle formation remain essentially unknown.

Several studies have demonstrated the importance of epithelial-endothelial interactions in organs developing from the endoderm (Hick et al., 2013; Lammert et al., 2001; Lazarus et al., 2011; Pierreux et al., 2010). In the thyroid, we found that endothelial cells are recruited in response to epithelial-derived Vegfa and are essential for the organization of the thyroid epithelial cell mass into follicles (Hick et al., 2013). However, the identity and mode of action of folliculogenic factor(s) are still unknown.

Bone morphogenetic proteins (BMPs) are members of the transforming growth factor beta (TGFβ) family that control many developmental processes such as epithelial differentiation and tissue morphogenesis (Macias et al., 2015). Upon BMP ligand binding to its receptor, the intracellular signal transducers Smad1/5/8 become activated by C-terminal phosphorylation. Phosphorylated Smad1/5/8 bind Smad4 and translocate to the nucleus where they regulate the expression of target genes, such as the Id genes. BMPs also interact with members of the apicobasal polarity complex, as exemplified by early events of neural tube closure (Eom et al., 2011). Loss of the twisted gastrulation (*Twsg1*) gene, which encodes a BMP modulator, causes craniofacial defects, affects foregut endoderm and reduces the expression of *Hhex*, a transcription factor required for early thyroid development (Petryk et al., 2004). Interestingly, reports on embryonic stem cell (ESC) differentiation have shown that modulation of BMP signaling is crucial for efficient lineage specification of Nkx2.1[+] endodermal progenitors (Green et al., 2011; Longmire et al., 2012; Kurmann et al., 2015).

Since Smads often function redundantly, we studied the role of BMP signaling in the thyroid gland by combined genetic inactivation of *Smad1* and *Smad5*. We found that the *Smad1* and *Smad5* double-knockout (*Smad1/5*[dKO]) mice have retarded growth, suffer from hypothyroidism and display a major perturbation in follicle development. Defective folliculogenesis, highly reminiscent of that observed in *Vegfa* knockout (*Vegfa*[KO]) mice, was associated with impaired assembly of basement membrane proteins and could be rescued by laminin-rich conditioned medium. Our results indicate that epithelial BMP-Smad1/5 signaling and endothelial

DEVELOPMENT

cells of the thyroid promote folliculogenesis via assembly of the basement membrane.

RESULTS
Active BMP signaling in thyrocyte progenitors during thyroid development
We first analyzed BMP signaling during normal thyroid development at the time of follicle formation (from E14.5 to E18.5). Most BMP ligands were expressed in the developing thyroid and, among these, *Bmp2*, *Bmp4*, *Bmp5* and *Bmp7* were the most abundant (Fig. 1A). Genes encoding BMP type I and type II receptors, intracellular Smad1, Smad5 and Smad8, as well as the common mediator Smad4, were also well expressed (Fig. 1A). Measurement of the absolute copy number of *Smad1/5/8* in E14.5 thyroid glands (Fig. 1B) showed that *Smad8* mRNA is only ~25% as abundant as *Smad1* and *Smad5*.

We next assessed whether BMP signaling is active during thyroid development. We first recorded *in vivo* BMP signaling activity in the thyroid region using a transgenic line expressing green fluorescent protein (GFP) under the control of BMP-responsive elements (BREs) (Monteiro et al., 2008). At E14.5, GFP expression was not detected in E-cadherin[+] thyroid epithelial cells, but was found in the parathyroid and in PECAM^{+} endothelial cells that form blood vessels running along and in between the thyroid epithelial cell masses (Fig. 1C). One day later, GFP was detected in some thyroid epithelial cells, and by E16.5 in almost all of the E-cadherin[+]/Tg^{+} cells (Fig. 1C). Conversely, GFP colocalization with PECAM was weak at that stage.

We further monitored phosphorylation of Smad1/5 (pSmad1/5) by whole-mount analysis of microdissected thyroid lobes (Fig. 1D). In untreated thyroid lobes, we could only detect pSmad1/5 at E15.5 in some E-cadherin[+] and E-cadherin^{−} cells. However, incubation of E14.5 and E15.5 thyroid lobes in Bmp4 induced Smad1/5 phosphorylation and nuclear translocation in epithelial cells (Fig. 1D). This indicated that thyroid epithelial cells are responsive to BMP signaling as early as E14.5 and that signaling is turned on in the developing thyroid between E14.5 and E15.5, i.e. at the start of, and during, follicle development.

Smad1/5[dKO] mice display growth retardation, abnormal follicles and hypothyroidism
To determine the role of BMP signaling in the thyroid, we deleted the most abundant Smads, namely Smad1 and Smad5, in the thyroid by crossing mice bearing conditional alleles of *Smad1* (*Smad1*^{fl/fl})
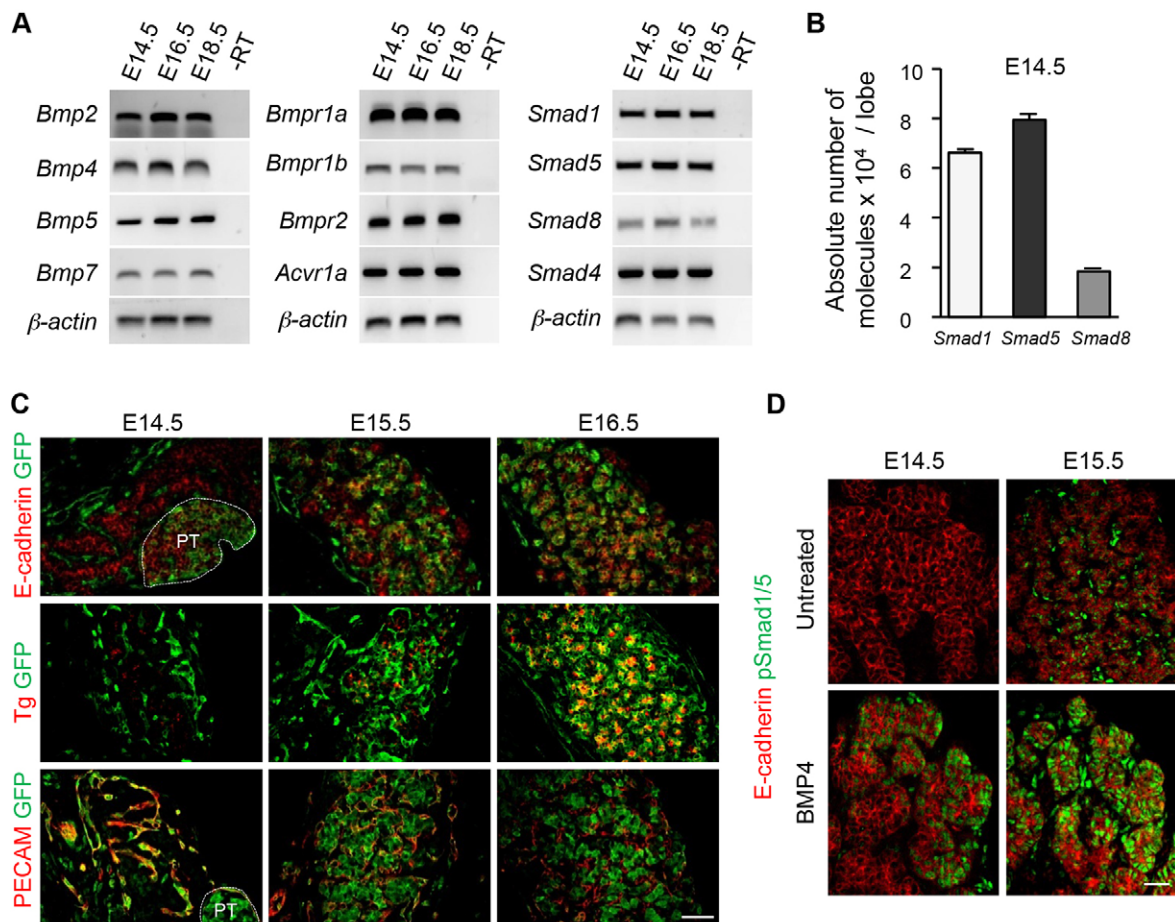
Fig. 1. Active BMP signaling in thyrocyte progenitors during thyroid development. (A) BMP ligands, receptors and Smad intracellular mediators are expressed in the mouse thyroid during follicle formation from E14.5 to E18.5. *Bmp2*, *Bmp4*, *Bmp5*, *Bmp7* are the most abundant mRNAs in the thyroid (*n*≥3). -RT, without reverse transcriptase. (B) Absolute quantification of *Smad1/5/8* mRNAs at the initiation of follicle development (E14.5) reveals that Smad1 and Smad5 are the most abundant intracellular mediators of BMP signaling in the thyroid (*n*≥3). (C) Thyroid sections from the BRE-GFP reporter mouse line reveal the presence of GFP (green) at E14.5 in blood vessels (PECAM) and parathyroid (PT; delineated by the white dotted line) but not in immunolabeled thyroid epithelial cells (E-cadherin). From E.15.5 onwards, most epithelial cells (thyroglobulin, Tg) of the developing thyroid display GFP activity. (D) Detection of pSmad1/5 is increased on sections of E14.5 and E15.5 explants treated for 30 min with 20 ng/ml Bmp4, as compared with untreated samples. Perfusion time probably explains the peripheral to central gradient of pSmad1/5. Data are presented as mean±s.e.m. Scale bars: 50 μm.

and *Smad5* (*Smad5*^{fl/fl}) with Pax8-Cre mice (Bouchard et al., 2004). Single-knockout (*Smad1*[KO] and *Smad5*[KO]) as well as double-knockout (*Smad1/5*[dKO]) mice were viable and born at normal Mendelian ratios. Only the *Smad1/5*[dKO] displayed a smaller body size and significantly reduced body weight at 10 weeks (Fig. 2A).

Histological analysis of control thyroids at 10 weeks showed a collection of large follicles composed of a monolayer of epithelial cells delineating a round lumen (Fig. 2Ba). *Smad1*[KO] and *Smad5*[KO] thyroid appeared comparable to that of the control, although the follicles in *Smad5*[KO] were somewhat smaller (Fig. 2Bb,c). In marked contrast, the thyroid structure of *Smad1/5*[dKO] was completely disorganized, with substantially fewer, irregular follicles delineated by taller thyrocytes (Fig. 2Bd). This was accompanied by adipogenesis in *Smad1/5*[dKO], which also occurred to a lesser extent in *Smad1*[KO] (data not shown). To evaluate thyroid function, we immunostained sections for iodinated Tg. This led to homogeneous staining filling the colloid of all follicles of control and single-knockout thyroids (Fig. 2Be-g). In *Smad1/5*[dKO], iodinated Tg was limited to a peripheral rim, suggesting colloid depletion due to high turnover rate (Fig. 2Bh). These data suggested that, although some thyroid differentiation can occur in *Smad1/5*[dKO], functionality was dramatically affected.

Because *Smad1/5*[dKO] displayed growth retardation and histological alterations of the thyroid glands, we next analyzed the thyroid hormonal status at 10 weeks. Plasma T_3 and T_4 concentrations were decreased by 80% in *Smad1/5*[dKO] (Fig. 2C) and, accordingly, thyroid-stimulating hormone (TSH) concentrations were dramatically increased up to 20,000-fold

(Fig. 2C). Thus, this major feedback response was insufficient to maintain plasma T_3 and T_4 concentrations (Fig. 2C), demonstrating thyroid unresponsiveness. Taken together, these data indicated that Smad1 and Smad5 are redundantly required for thyroid follicle formation and function.

Smad1/5 are efficiently inactivated in thyrocyte progenitors

The severe follicular alterations and major hypothyroidism of adult *Smad1/5*[dKO] mice suggested that follicle formation and/or differentiation might be affected in embryonic thyroid. We first verified Cre-mediated *Smad1* and *Smad5* recombination by measuring the abundance of *Smad1/5/8* mRNA during early stages of embryonic thyroid development (Fig. 3A). Compared with controls, *Smad1/5*[dKO] thyroid showed a 50% reduction in the abundance of *Smad1* and *Smad5* mRNA as early as E14.5, and this reduction persisted until the end of gestation (Fig. 3A). *Smad8* expression, used as a control Smad, was not affected at E14.5 or E16.5. Surprisingly, its level was significantly decreased at E18.5, suggesting positive regulation by BMP-Smad1/5 signaling during thyroid development. Based on epithelial-specific Pax8-Cre expression, we hypothesized that the 50% global reduction in *Smad1/5* reflected loss of expression in the developing thyrocytes but persistent expression in other cell types. Further, treating cultured thyroid lobes with Bmp4 revealed phosphorylation of Smad1 and Smad5 in control but not in the vast majority of *Smad1/5*[dKO] epithelial cells (Fig. 3B). These data indicated that Smad1/5 were successfully inactivated in thyroid epithelial cells and suggest that the remaining 50% expression in
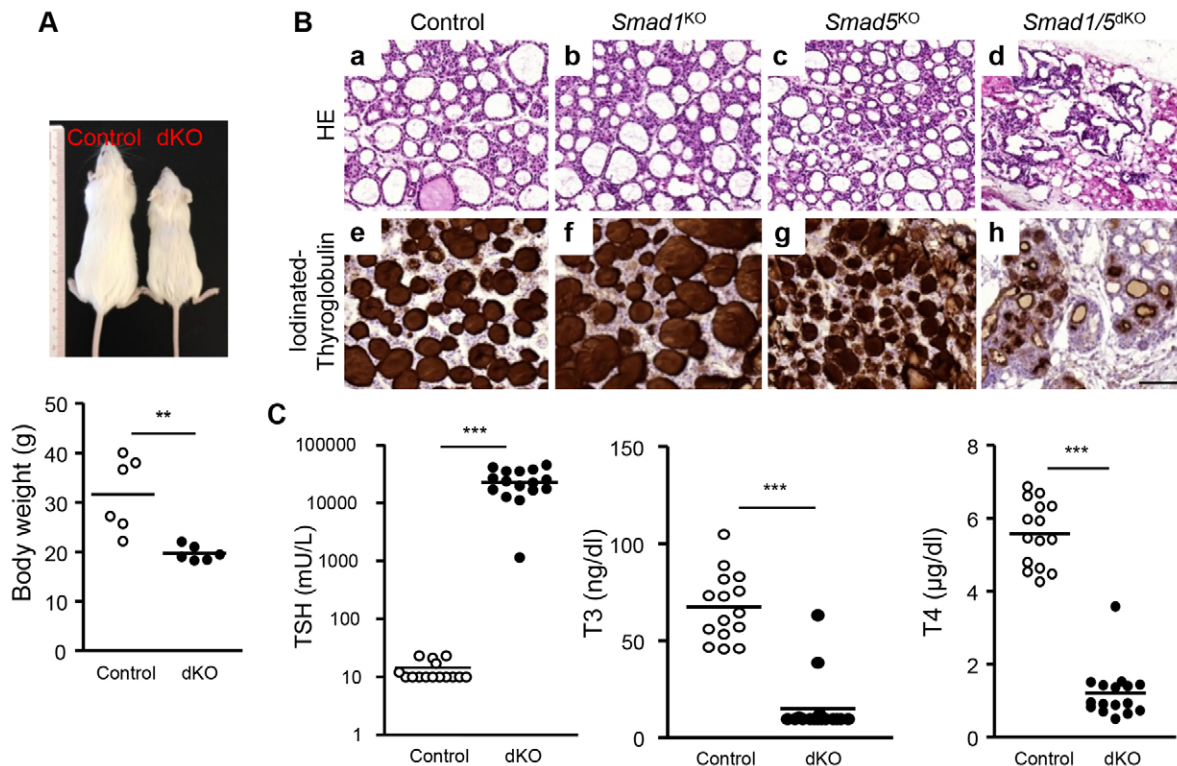
Fig. 2. Smad1/5[dKO] mice display growth retardation, abnormal follicles and hypothyroidism. Ten-week-old single- and double-knockout mice were compared with age-matched controls. (A) *Smad1/5*[dKO] mice are of smaller body size and lower body weight compared with control. (B) H&E staining of control (a), *Smad1*[KO] (b) and *Smad5*[KO] (c) thyroids reveals abundant mature follicles lined with flat thyrocytes, whereas *Smad1/5*[dKO] (d) exhibits severe disorganization of the thyroid parenchyma, with fewer and abnormal follicular structures lined with thicker thyrocytes, suggesting an abnormally high TSH level. Control (e), *Smad1*[KO] (f) and *Smad5*[KO] (g) thyroids show homogeneous and dense signal for iodinated Tg in the colloid, whereas in the *Smad1/5*[dKO] (h), iodinated Tg is limited to a peripheral rim. (C) TSH, T_3 and T_4 concentrations were measured in plasma of control and *Smad1/5*[dKO] mice ($n \geq 15$). Most *Smad1/5*[dKO] mice exhibit very high plasma or serum TSH and low T_3 and T_4. **$P<0.001$, ***$P<0.0001$, Mann–Whitney U-test. Data are presented as mean±s.e.m. Scale bar: 100 μm.
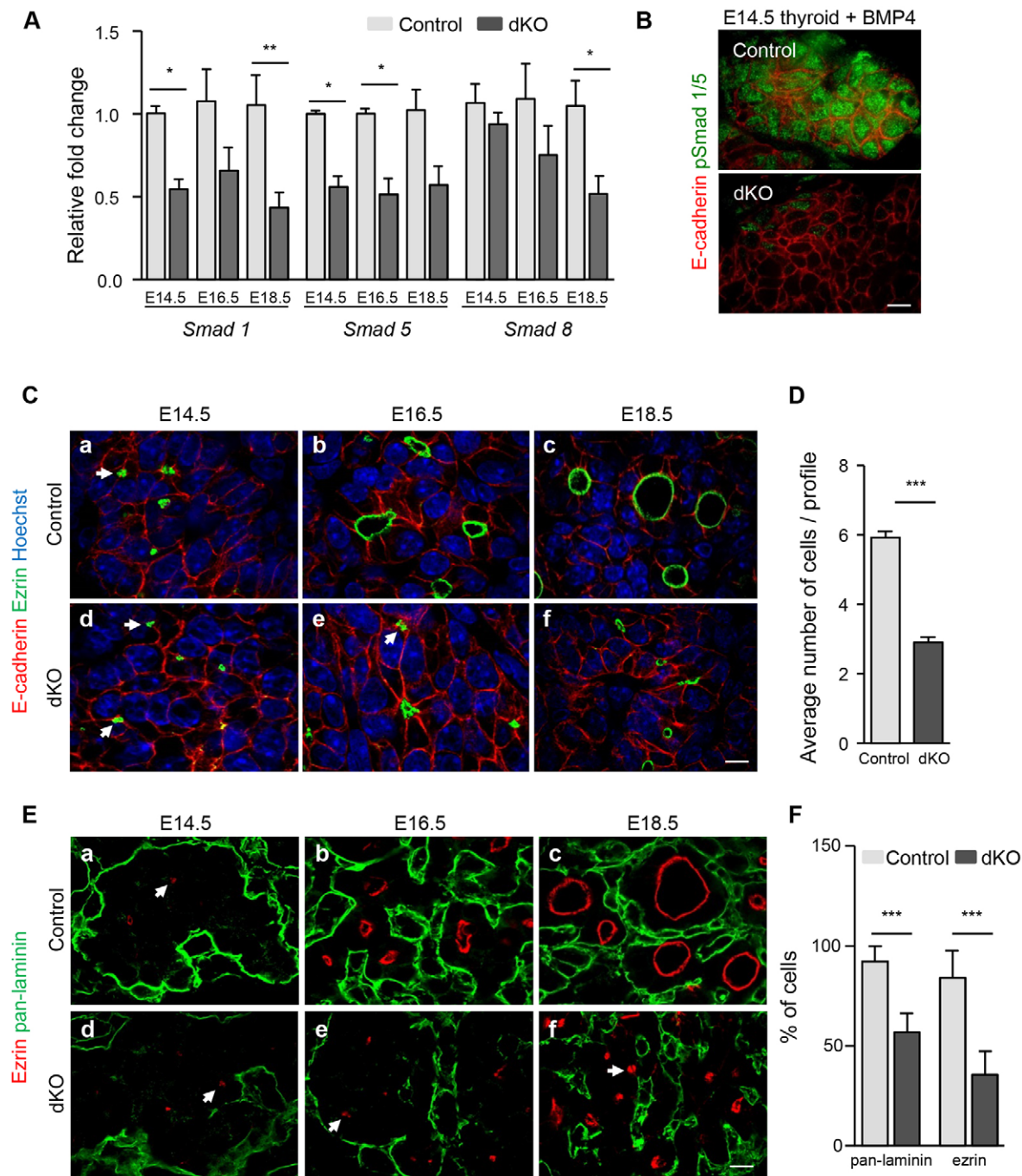
Fig. 3. Smad1/5 are efficiently inactivated in thyrocyte progenitors. (A) Compared with control thyroid lobes, *Smad1/5*^dKO^ show a ~50% reduction in *Smad1* and *Smad5* mRNA levels from E14.5 onwards. Expression of *Smad8* is affected at E18.5 (*n*≥5). (B) pSmad1/5 labeling reveals Smad activation in control but not in *Smad1/5*^dKO^ thyroid lobes at E14.5 treated in parallel with 20 ng/ml Bmp4. (C) Organization of epithelial progenitor cells (E-cadherin) in monolayers surrounding a lumen (ezrin) is impaired in *Smad1/5*^dKO^ thyroid glands. Arrows indicate ezrin^+^ structures in adjacent cells. (D) The number of cells per luminal profile of well-defined Par3^+^ structures (*n*≥13) is decreased by about half in thyroid glands of *Smad1/5*^dKO^ as compared with control. (E) Defective apical (ezrin) and basal (pan-laminin) specification in *Smad1/5*^dKO^, as compared with control thyroid glands. Arrows indicates ezrin^+^ structures in adjacent cells. (F) The number of cells in contact with pan-laminin and with ezrin is decreased in *Smad1/5*^dKO^. *P<0.05, **P<0.001, ***P<0.0001, Mann–Whitney U-test. All mRNAs were normalized to *Rpl27*. Data are presented as mean±s.e.m. Scale bars: 10 μm. See also Fig. S1.

the thyroid can be attributed to other cell types where Cre is not induced.

Smad1/5 inactivation impairs thyroid folliculogenesis

Follicle formation from an original mass of non-polarized epithelial cells involves a complex morphogenetic process

starting at ~E14.5. Careful analysis of thyroid gland development reveals progressive fragmentation of the epithelial mass, organization of the epithelial cells in independent spherical structures or rosettes, acquisition of apicobasal polarity and finally lumen expansion (Fagman et al., 2006; Hick et al., 2013). To determine when BMP signaling impacts on follicle formation, we

analyzed thyroid development in control and $Smad1/5^{dKO}$ mouse embryos from E14.5 to E18.5 (Fig. 3C,E).

In controls, punctate immunofluorescent labeling for the apical marker ezrin first became apparent in the thyroid mass at E14.5, just underneath or fused with the membrane of epithelial progenitors (Fig. 3Ca). We interpret these puncta as ezrin-coated vesicles en route to predefined plasma membrane domains in order to initiate apical pole formation. In sections we frequently observed two such vesicles closely apposed, face to face, next to the plasma membrane of adjacent cells (arrows in Fig. 3C,E). At this stage, the basal marker laminin was only found between thyroid peripheral cells and the stroma (Fig. 3Ea). By E16.5, coordinated fusion of vesicles from several epithelial cells initiated the creation of small lumina. Thyrocyte progenitors organized in microfollicles progressively assembled a laminin-rich basement membrane, appearing as a dense meshwork that fragmented the mass (Fig. 3Cb,Eb). By the end of gestation, most follicular structures were individualized, i.e. each completely surrounded by laminin (basal pole) and enclosing an expanded lumen circumscribed by ezrin$^+$ membrane (apical pole) (Fig. 3Cc,Ec).

In the absence of Smad1 and Smad5, the thyroid mass at E14.5 was delineated by a single laminin shell and thyroid epithelial cells contained small puncta of ezrin, as in wild-type controls (Fig. 3Cd,Ed). By E16.5, fusion of ezrin$^+$ vesicles with the membrane also occurred, but the lumina of microfollicles were much smaller than in wild type (Fig. 3Ce,Ee). In addition, there was a 50% reduction in epithelial cells showing ezrin$^+$ membrane (83.9± 13.8% in wild type versus 35.5±11.7% in $Smad1/5^{dKO}$; Fig. 3F). Fragmentation of the thyroid mass was also impaired: a large fraction of epithelial cells remained associated in large clusters so that their contact with the basement membrane (pan-laminin) was reduced by about half (92.2±7.7% in wild type versus 56.7±9.5% in $Smad1/5^{dKO}$; Fig. 3F). By E18.5, the difference between control and $Smad1/5^{dKO}$ was even more evident. Most epithelial cells remained associated, microfollicles were composed of a reduced number of cells, were only partially delineated by laminin and their lumen did not appreciably expand (Fig. 3Cf,Ef,D). Quantification of sectioned lumen size revealed a 4-fold difference in $Smad1/5^{dKO}$ compared with control (33.9±2.9 μm^2 in $Smad1/5^{dKO}$ versus 137.1±11.2 μm^2 in wild type), thus an 8-fold difference in volume. However, the global thyroid size, the thyrocyte proliferation rate and the number of open ezrin$^+$ structures were not affected by Smad1/5 inactivation (data not shown). Altogether, these results indicated that BMP signaling is essential for epithelial reorganization of the thyroid progenitor mass into follicles with large lumina.

Despite the reduced number of ezrin$^+$ epithelial cells and the smaller lumina, we noticed that, when present, ezrin was correctly localized to the apical pole in $Smad1/5^{dKO}$. This suggested that apical polarity was preserved in these cells. To further test this interpretation, we analyzed control and $Smad1/5^{dKO}$ thyroid for Par3, a key component of the apical polarization machinery, and F-actin for cytoskeleton organization, and found no obvious difference between controls and $Smad1/5^{dKO}$ (Fig. S1A). Furthermore, transmission electron microscopy revealed that epithelial cells involved in immature microfollicles in $Smad1/5^{dKO}$ still developed tight junctions and microvilli projecting into the lumen space, as in control follicles (Fig. S1B). However, intracellular microvilli inclusion bodies were observed in $Smad1/5^{dKO}$, suggesting defective apical delivery of intracellular vesicles (Fig. S1B, inset).

Altogether, these data indicated that BMP-Smad signaling controls folliculogenesis downstream of the initial apical specification but upstream of basement membrane assembly, epithelial reorganization and lumen expansion.

Smad1/5 signaling in thyrocytes stimulates *Vegfa* expression and affects gene expression in neighboring endothelial cells

Previous work from our group has shown that endothelial cell recruitment into the developing thyroid is required for follicle formation. The folliculogenic effect of endothelial cells was contact independent and could be mimicked with medium conditioned by endothelial cells (Hick et al., 2013). We thus tested whether the defective folliculogenesis in $Smad1/5^{dKO}$ could be due to a lack of either endothelial cells or a signal derived therefrom. We identified endothelial cells by immunofluorescence for PECAM (Pecam1), a cell adhesion molecule specifically expressed by endothelial cells, in control and $Smad1/5^{dKO}$ thyroids from E14.5 to E18.5 (Fig. 4A). In control and $Smad1/5^{dKO}$ thyroids, the abundance and localization of blood vessels were unaffected at the three stages analyzed (Fig. 4A). Quantification of endothelial sectioned surface and the epithelial-to-endothelial sectioned surface ratio did not reveal any significant differences between $Smad1/5^{dKO}$ and the control.

To evaluate endothelial cell differentiation in $Smad1/5^{dKO}$, we measured the expression of selected endothelial-specific genes. Expression of vascular endothelial cadherin [cadherin 5 (*Cdh5*)] and vascular endothelial cadherin 2 [protocadherin 12 (*Pcdh12*)] as well as of *Tie1* was significantly reduced at E16.5 (Fig. 4B), but expression of *Vegfr2*, *Pecam1* and endothelial cell-specific molecule 1 (*Esm1*) was normal. *Vegfa* controls endothelial cell development and BMP-Smad1/5 signaling is known to control *Vegfa* expression in several cell types (Bai et al., 2013; Deckers et al., 2002; Shao et al., 2009; Shimizu et al., 2012). We measured *Vegfa* in developing $Smad1/5^{dKO}$ thyroids and found that it was reduced starting at E14.5; this reduction reached statistical significance starting at E16.5 (Fig. 4C). We thus directly analyzed the effect of BMP addition on *Vegfa* expression in microdissected thyroid lobes at E14.5 and in the thyroid follicular cell line FRTL-5. Treatment of thyroid lobes with the specific BMP inhibitor DMH1 (Hao et al., 2010) led to a reduction in expression of *Vegfa* and of the BMP-Smad1/5 signaling target gene *Id2* (Fig. 4D). Incubation of wild-type thyroid lobes with BMP ligands induced *Id2*, but did not modify the already high *Vegfa* expression (Hick et al., 2013). To circumvent any BMP accessibility issues, we incubated the thyroid cell line FRTL-5 with a combination of the most abundant BMP ligands in the thyroid (Bmp2, 4, 5 and 7) and noticed a dose-dependent stimulation of the expression of *Vegfa* and *Id2* (Fig. 4E). These results indicated that epithelial Smad1/5 signaling regulates *Vegfa* and endothelial gene expression.

Production of the basement membrane proteins laminin and type IV collagen is decreased in *Smad1/5*^{dKO} and *Vegfa*^{KO} thyroid glands

We next turned to the identification of the follicle-promoting factor(s). Knowing that thyrocytes and endothelial cells form their own continuous basement membrane, that extracellular matrix components promote epithelial cell organization, and that contact with laminin was partly impaired in $Smad1/5^{dKO}$, we postulated that the basement membrane could stimulate folliculogenesis. To test this hypothesis, we first looked for a possible defect in laminin and type IV collagen expression in $Smad1/5^{dKO}$ and $Vegfa^{KO}$ (Fig. S2). Laminins are a family of five α, three β and three γ chains forming αβγ heterotrimers that span the basement membrane. The collagen
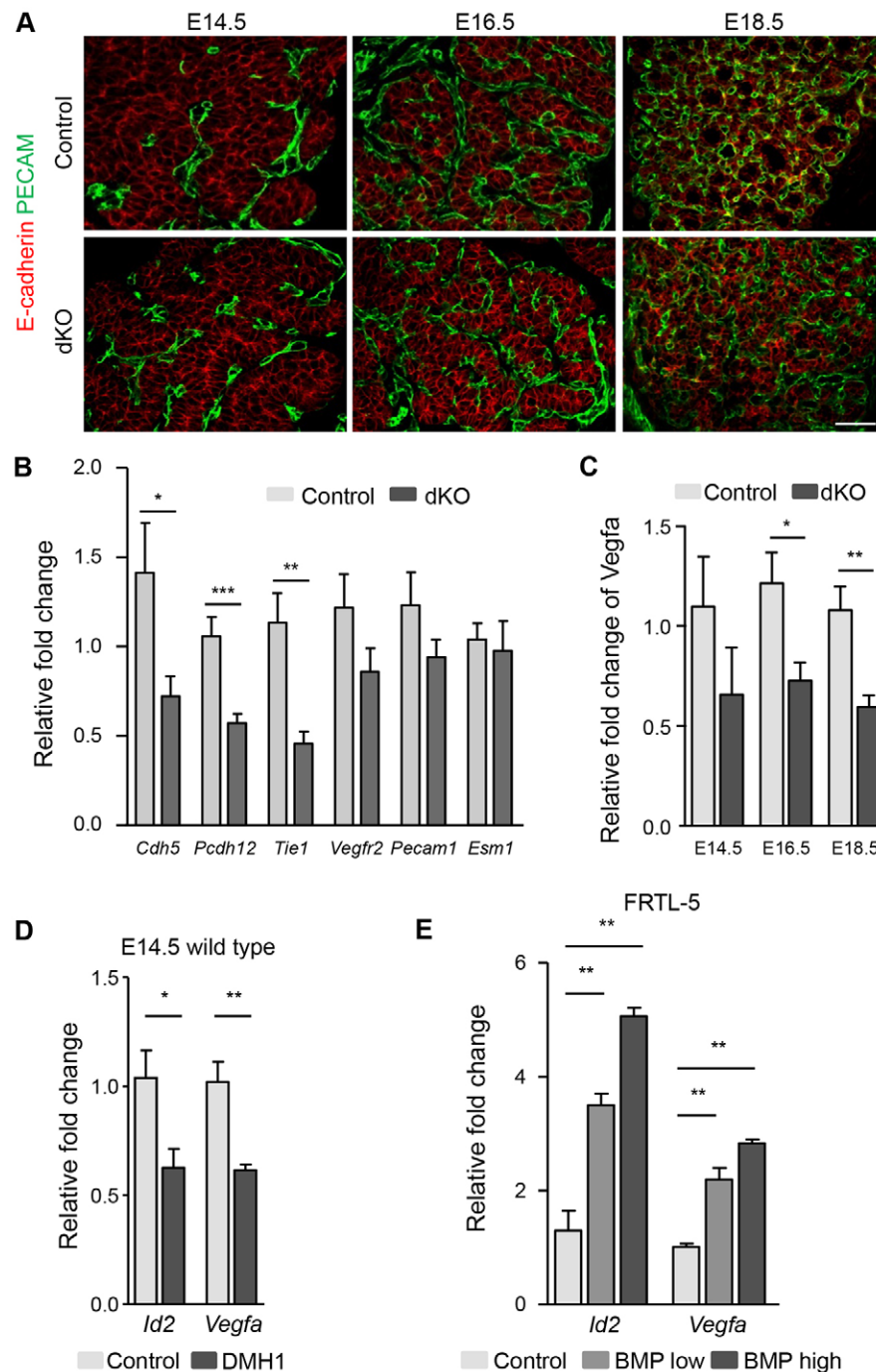
Fig. 4. Normal blood vessel density but altered *Vegfa* and endothelial cell gene expression upon Smad1/5 inactivation. (A) Immunolabeling for E-cadherin and PECAM reveals preserved blood vessel density in *Smad1/5*^dKO mice from E14.5 to E18.5. (B) Expression of *Cdh5*, *Pcdh12* and *Tie1* is significantly reduced after epithelial inactivation of Smad1/5 at E16.5. (C) *Vegfa* expression is reduced in *Smad1/5*^dKO thyroid as compared with control. (D) E14.5 thyroid lobes treated with 3 μM DMH1 (BMP inhibitor) for 16 h have reduced *Id2* and *Vegfa* mRNA levels. (E) Expression of *Id2* and *Vegfa* in FRTL-5 cells is rapidly (8 h) stimulated by a mix of Bmp2, 4, 5, 7 ligands in a dose-dependent manner. *P<0.05, **P<0.001, ***P<0.0001, Mann–Whitney U-test (n≥5). All mRNAs were normalized to either *Rpl27* or *Actb*. Data are presented as mean±s.e.m. Scale bar: 50 μm.

type IV family has six α chains forming trimers interconnected with the laminin network.

In *Smad1/5*^dKO, expression of laminin α2, α3, β1 and β3 chains was significantly, albeit transiently, reduced (Fig. S2A,B). Expression of laminin α3 and α4 was significantly reduced in *Vegfa*^KO (Fig. S2C). Of note, laminin α4 displays an endothelial-specific pattern in E16.5 embryos (The Matrixome Project, Osaka University, Japan). A similar analysis revealed a reduction of most type IV collagen genes in *Smad1/5*^dKO (Fig. S2D). There was a substantial and sustained reduction in collagen α3-6(IV) chains. Collagen α1(IV) and α2(IV) were modestly reduced or delayed. In *Vegfa*^KO, expression of collagen α1(IV) and α2(IV) was significantly reduced (Fig. S2E); both genes were also reported as

endothelial specific (The Matrixome Project). In conclusion, gene expression analysis revealed decreased expression of several basement membrane proteins in *Smad1/5*^dKO and *Vegfa*^KO.

We next examined by immunofluorescence whether decreased gene expression resulted in impaired basement membrane assembly. In line with the gene expression analysis, collagen type IV signals were severely affected in both *Smad1/5*^dKO and *Vegfa*^KO (Fig. 5Ab,d). Pan-laminin signals were also reduced in *Smad1/5*^dKO, and only modestly in *Vegfa*^KO (Fig. 5Af,h). Taken together, these data indicated that expression and/or deposition of basement membrane proteins depends on endothelial cells and Smad1/5 signaling in thyrocytes, and suggested an essential role for basement membrane assembly in folliculogenesis.
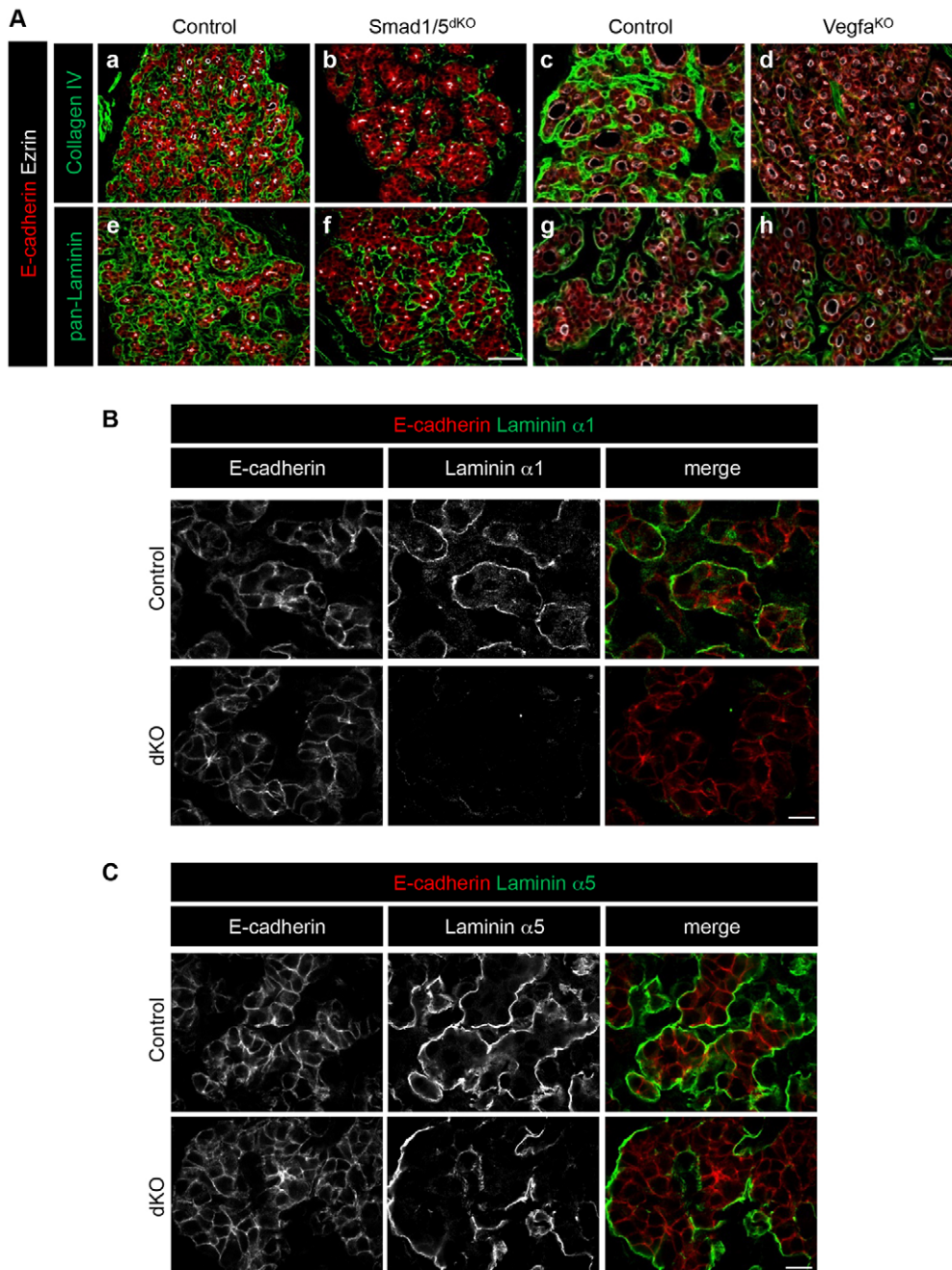
Fig. 5. Production of the basement membrane proteins laminin and type IV collagen, is decreased in *Smad1/5*^{dKO} and *Vegfa*<sup>KO</sup> thyroid glands. Thyroid gland sections from *Smad1/5*^{dKO} at E16.5 and *Vegfa*^{KO} at P0 were analyzed by immunolabeling for basement membrane markers and compared with age-matched control thyroid. (A) Comparative multiplex immunolabeling for thyrocyte epithelial E-cadherin, the polarity marker ezrin and the basal markers pan-laminin or type IV collagen. Type IV collagen signal is decreased in *Smad1/5*^{dKO} and *Vegfa*^{KO}. Pan-laminin signal shows subtle changes when compared with that in control mice. (B) Immunolabeling of laminin α1, as found around epithelial cells (E-cadherin) in control, is markedly decreased in *Smad1/5*^{dKO} at E16.5. (C) Immunolabeling of laminin α5, as found around epithelial cells (E-cadherin) in control, is marginally affected in *Smad1/5*^{dKO} at E16.5. Scale bars: 50 μm in A; 10 μm in B,C. See also Figs S2 and S3.

Epithelial laminin production is affected in *Smad1/5*^{dKO}

Mature angiofollicular units are characterized by close proximity between endothelial and epithelial cells. To determine the respective contribution of epithelial and endothelial cells to basement membrane protein synthesis, we analyzed the expression of laminin and collagen type IV genes in FACS-sorted epithelial populations (Fig. S3). Epithelial thyrocyte progenitors were selected based on YFP expression after Pax8-Cre-mediated recombination of the ROSA-STOP-YFP locus. This population was compared with YFP^{−} cells, which thus included C-cells, endothelial and mesenchymal cells but also non-recombined thyrocyte progenitors. *Yfp* mRNA was only found in the YFP⁺ cells. *Pax8* and the epithelial marker E-cadherin showed a 2-fold enrichment in this population, while *Vegfr2* was enriched 4-fold in the YFP[−] population, as expected (Fig. S3A). mRNAs for all

collagen type IV genes as well as laminins α3, β1-3 and γ1,2 were equally distributed in YFP⁺ and YFP^{−} thyroid cells. By contrast, laminin α1 and α5 chains were enriched in the YFP⁺ epithelial population, whereas laminin α2 and α4 chains showed the strongest expression in the YFP[−] population (Fig. S3B).

Since laminins α1 and α5 were enriched in the epithelial population, we studied their expression by immunofluorescence using isoform-specific antibodies. In control thyroid glands, epithelial follicular structures were surrounded by almost continuous laminin α1 and α5 signal. In *Smad1/5*^{dKO} thyroids, laminin α1 signal was severely reduced (Fig. 5B), supporting the RT-qPCR analysis (Fig. S2A). Laminin α5 signal was comparable to that of controls, although the pattern was affected owing to the epithelial organization defect (Fig. 5C). These data confirmed that the key basement membrane proteins, laminin and collagen type IV,
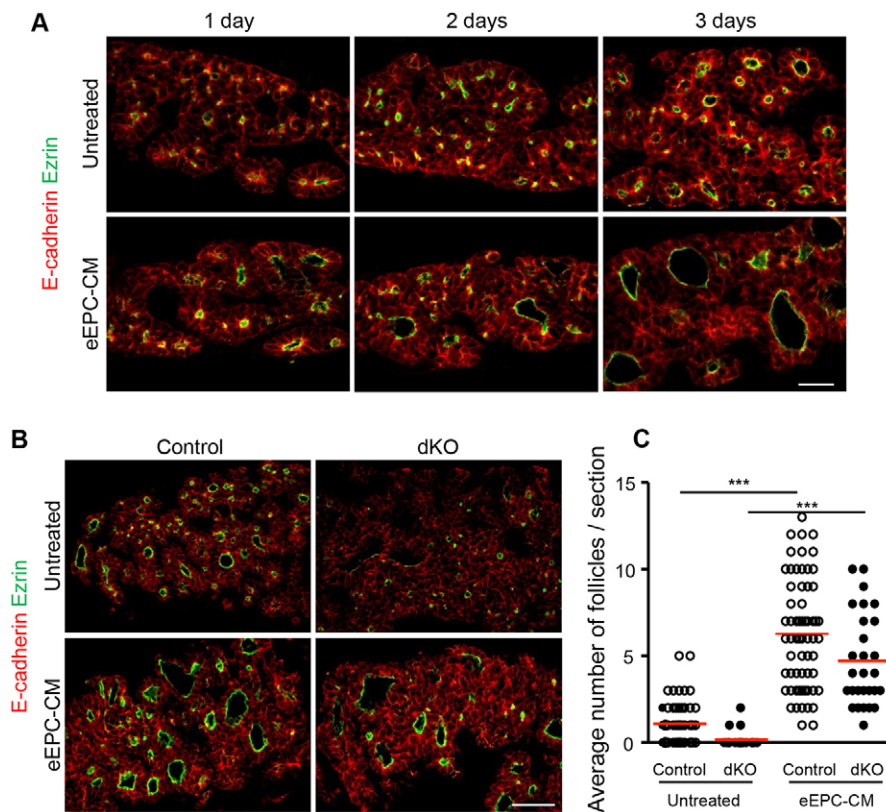
Fig. 6. Medium conditioned by endothelial cells contains folliculogenic factor(s) and rescues the follicle formation defect of *Smad1/5*[dKO]. (A) Within 3 days of culture, epithelial cells (E-cadherin) from wild-type E14.5 thyroid lobes polarize apically (ezrin) and form small follicles. Addition of eEPC-CM to the culture stimulates polarization and follicle formation. (B) Compared with control, ezrin[+] structures are smaller in untreated *Smad1/5*[dKO] thyroid lobes, but are enlarged when cultured with eEPC-CM. (C) The number of large ezrin[+] luminal follicles per thyroid explant section was calculated. ***$P<0.0001$, one-way ANOVA followed by Bonferroni's multiple comparison test ($n \geq 23$). Data are presented as mean±s.e.m. Scale bars: 20 µm in A; 50 µm in B. See also Fig. S4.

are produced by both epithelial and endothelial components of the angiofollicular units, and indicated that *Smad1/5*[dKO] epithelial cells have an impaired ability to produce and assemble laminin α1-containing heterotrimers.

Medium conditioned by endothelial cells contains folliculogenic factor(s) and rescues the follicle formation defects of *Smad1/5*[dKO] and *Vegfa*[KO]

To investigate the mechanism of follicle formation, we resorted to an *ex vivo* culture system of thyroid lobes. We had previously reported that pharmacological ablation of endothelial cells in E12.5 thyroid explants prevented folliculogenesis; conversely, addition of medium conditioned by embryonic endothelial progenitor cells (eEPCs), herein referred to as eEPC-CM, was able to rescue, and even overstimulate, follicle formation (Hick et al., 2013). Using an improved thyroid lobe culture system (Delmarcelle et al., 2014), we found that addition of eEPC-CM to non-ablated wild-type thyroid lobes promotes follicle development by up to 6-fold after 3 days of culture (Fig. 6A,C). This medium thus contains folliculogenic factor(s).

We then addressed whether eEPC-CM could rescue the defective folliculogenesis of *Smad1/5*[dKO] and *Vegfa*[KO]. We first verified that E14.5 *Smad1/5*[dKO] thyroid lobes reproduce impaired follicle formation upon *ex vivo* culture: only very small ezrin[+] structures could be observed after 3 days (Fig. 6B). Importantly, eEPC-CM significantly induced follicle formation in *Smad1/5*[dKO] thyroid lobes (Fig. 6B,C), and the same was found for *Vegfa*[KO] (Fig. S4). The similar rescue of immature microfollicle development of *Smad1/5*[dKO] and *Vegfa*[KO] thyroid glands by folliculogenic factor(s) in eEPC-CM suggested that these factor(s) act downstream of epithelial Smad1/5 signaling and of endothelial cell invasion.

Laminins deposited and assembled around thyroid epithelial cells promote folliculogenesis

Among potential folliculogenic factors, we examined whether eEPCs expressed and released basement membrane proteins into their CM. We first determined the expression profile of laminin subunit and collagen type IV genes in eEPCs. We found that eEPCs express very high levels of laminin α1, β1 and γ1 mRNAs, which almost reached the level of the β-actin (*Actb*) housekeeping gene (Fig. 7A). Among collagen type IV genes, α6 showed the highest level of expression, albeit ~1000× lower than laminin β1.

We next verified that eEPCs can secrete laminins into the CM, in particular laminin-111 (heterotrimer of α1, β1 and γ1), by silver staining, western blotting and mass spectrometry. Silver staining after SDS-PAGE of CM revealed a well-defined band migrating at a similar M_r to purified laminin-111 (Fig. 7B). Western blotting with laminin α1-specific antibody identified this subunit (Fig. 7B). Mass spectrometry further easily detected laminin α1, β1 and γ1 peptides in the CM (Table S1). Finally, we asked whether laminin-111 from eEPC-CM was deposited on cultured E14.5 thyroid lobes. Immunofluorescence for laminin α1 revealed a much stronger signal after 1 day of incubation with the CM as compared with untreated explants. This signal further increased after 2 and 3 days of culture and became organized around peripheral epithelial structures (Fig. 7C). These data indicated that laminin-111, which is expressed and secreted by eEPCs into the medium, can be assembled around epithelial structures of thyroid lobes.

To confirm that laminin-111 acts as a folliculogenic factor, we inhibited its production in eEPCs. Silencing laminin α1 in eEPCs by shRNA yielded CM that was abrogated in its folliculogenic activity on thyroid lobes (Fig. 7D,E), while preventing the accrued deposition of laminin α1 in thyroid lobes (Fig. 7E). Similar
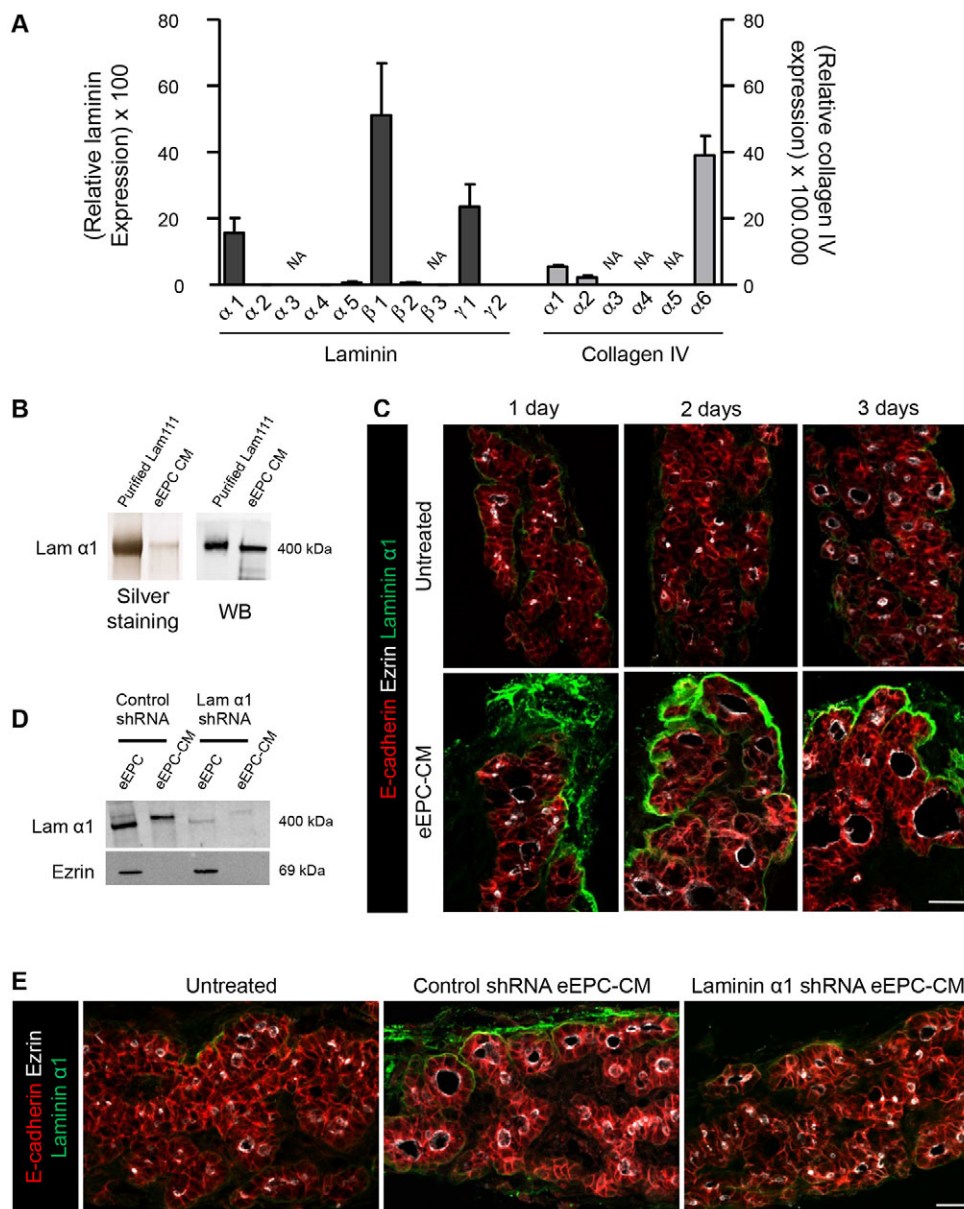
Fig. 7. Laminins deposited and assembled around thyroid epithelial cells promote folliculogenesis. (A) eEPCs express high level of selected laminin genes and much lower levels of collagen IV genes. All mRNAs were normalized to *Actb*. Data are presented as mean±s.e.m. ($n \geq 3$). NA, non-amplified. (B) Laminin $\alpha 1$ (400 kDa) is secreted by eEPCs and accumulates in eEPC-CM. WB, western blot. (C) E14.5 thyroid lobes cultured with eEPC-CM show intense signal for laminin $\alpha 1$ around thyroid epithelial cells (E-cadherin) and show larger follicles (ezrin) as compared with untreated lobes. (D) shRNA-mediated laminin $\alpha 1$ silencing in eEPCs decreases laminin $\alpha 1$ in eEPC extract and in eEPC-CM, as compared with control shRNA. Ezrin is used as a loading control for eEPC extracts. (E) Compared with thyroid lobes cultured with CM from control shRNA-treated eEPCs, lobes cultured in the presence of CM from laminin $\alpha 1$ shRNA-treated eEPCs do not show laminin $\alpha 1$ deposition and have small follicles, similar to those of untreated lobes. Scale bars: 20 μm.

results were obtained upon laminin β1 and γ1 silencing (data not shown). These data indicated that laminin-111 in eEPC-CM is a key actor of thyroid folliculogenesis.

DISCUSSION

Here, we examined if and how BMP-Smad signaling is required for thyroid follicle formation. We found that BMP signaling was activated in thyroid epithelial cells during folliculogenesis. Inactivation of Smad1/5 in thyroid epithelium caused major alterations to follicular structures, hypothyroidism and growth retardation but no loss of viability. Defective follicular development was associated with impaired basement membrane assembly, highly reminiscent of the folliculogenesis defect of *Vegfa*[KO] embryos in which endothelial cells are, however, absent. Follicle formation defects in *Smad1/5*[dKO] and *Vegfa*[KO] could be rescued with laminin-rich CM. Taken together, our findings support a model in which thyroid follicle formation depends on basement membrane assembly, a process controlled by epithelial Smad1/5 signaling and endothelial cells.

Ten-week-old *Smad1/5*[dKO] mice were smaller and of reduced body weight compared with control littermates. Failure to grow is readily explained by the very low levels of thyroid hormones T_3 and T_4 and the extremely high TSH values, which demonstrated non-compensated hypothyroidism. Thyroid unresponsiveness despite huge TSH values is well known in mouse knockouts for the TSH receptor (*Tshr*), *Nkx2.1*, *Foxe1* and *Pax8* (De Felice and Di Lauro, 2004). *Smad1/5*[dKO] thyroid lobes were normal in size at birth, and the functional impairment of adult thyroid probably results from the embryonic folliculogenesis defects. However, we cannot exclude a role for BMP signaling in postnatal thyroid homeostasis.

Our laboratory has provided evidence that follicle formation occurs by reorganization of the thyroid primordium epithelial cell mass into polarized monolayers surrounding a central lumen, which is comparable to the cord hollowing model of *de novo* lumen formation (Andrew and Ewald, 2010) and the process of apicobasal polarization with lumen formation, as observed in MDCK cells when cultured in a 3D Matrigel. In this 3D culture system, fusion of vesicles to the apical membrane initiation site (AMIS) allows apical

DEVELOPMENT

lumen opening and cyst formation (Bryant et al., 2010). In the thyroid, we also observed pre-apical intracellular vesicles (ezrin[+]) and their coordinate exocytosis to generate apical lumen. Immature microfollicles can then expand or enlarge, while segregating from adjacent microfollicles and becoming vascularized by invading endothelial cells. In Smad1/5[dKO], despite the formation of ezrin[+] vesicles in some cells and endothelial invasion, the exocytosis of vesicles with membranes and lumen expansion were clearly impaired, as was fragmentation of the mass, leading to the individualization of microfollicles.

The occurrence of immature microfollicles in Smad1/5[dKO] thyroid suggests that the basal machineries for apical polarization and for the creation of secluded lumina are preserved. However, this does not mean that these machineries are quantitatively fully operative. Indeed, we found that substantially fewer epithelial cells participate in microfollicle formation (Fig. 3D), develop an ezrin[+] apical pole (Fig. 3F) and assemble a laminin[+] basal pole (Fig. 3F). Altogether, these data indicate that, although some epithelial cells in Smad1/5[dKO] thyroid engage in polarization and the formation of a secluded lumen, substantially fewer participate in this concerted process when BMP signaling is inactivated. These observations suggest either that BMP signaling is not required for apical polarization or that the genetic inactivation using Cre recombinase is not 100% effective in all Pax8^{+} cells at the same time and for all four Smad alleles.

Progression of immature microfollicles into larger structures, as clearly affected in Smad1/5[dKO], cannot be explained by impaired epithelial proliferation (normal rate in Smad1/5[dKO]). Conceivably, impaired follicle enlargement could be related to defective differentiation and thus a lower accumulation of Tg that would otherwise force expansion of the colloid lumen. However, Vegfa[KO] mice, which also display immature microfollicles, express Tg at an almost normal level (90% of wild type; Hick et al., 2013). This argues that Tg accumulation is not sufficient for lumen expansion. Comparison of Smad1/5[dKO] and Vegfa[KO] rather suggests that lumen enlargement depends on correct apicobasal polarization. Indeed, as compared with aged-matched control littermates, we found in both Smad1/5[dKO] and Vegfa[KO] reduced basement membrane deposition and the persistence of intracellular ezrin[+] vesicles, suggesting a relationship between basement membrane-triggered polarization and impaired fusion with the apical membrane (Fig. S1B and Fig. 3C,E, arrows).

The impaired follicle formation observed in the absence of Smad1 and Smad5 is reminiscent of the defect observed in the absence of endothelial cells upon Vegfa inactivation in thyroid epithelium (Hick et al., 2013). Although endothelial cell density in epithelial-specific Smad1/5[dKO] was comparable to that of control thyroid glands, expression of endothelial cell identity markers (Cdh5, Pcdh12 and Tie1) and endothelial-enriched basement membrane proteins (type IV collagen α1, α2 and laminin α3) was impaired, consistent with ongoing reciprocal paracrine communications between epithelial and endothelial cells (Hick et al., 2013). In this report, we further found that BMP-Smad signaling in thyroid epithelial cells controls the expression of Vegfa, in agreement with reports in other cell types (Bai et al., 2013; Deckers et al., 2002; Shao et al., 2009; Shimizu et al., 2012). Of note, this regulation in zebrafish could be either positive (for Smad1) or negative (for Smad5) (He and Chen, 2005). Our findings in developing thyroid suggest instead that BMPs could control the endothelial gene expression program indirectly, i.e. by regulating Vegfa expression. Changes in gene expression in endothelial cells could in turn impact on follicle formation. Several studies have

emphasized the crucial role played by endothelial cells via angiocrine factors in the regulation of organ morphogenesis (Ramasamy et al., 2015). Integrating available knowledge supports a reciprocal paracrine communication in which thyrocyte progenitors, under the influence of BMP, participate in the recruitment and maturation of thyroid endothelial cells, via Vegfa. In turn, endothelial cell invasion and maturation in the thyroid mass would create a microenvironment permissive for folliculogenesis.

The importance of the extracellular environment for cell polarization in tissue culture experiments has long been recognized (Wang et al., 1990a,b). Culture of MDCK epithelial cells in collagen-rich gel or Matrigel triggers the production of laminin and assembly of a basement membrane, which in turn promotes cystic structures (Bryant et al., 2010), a process that can be directly compared to the formation of thyroid follicles. In addition, ESCs, when forced to transiently co-express transcription factors Pax8 and Nkx2.1, differentiate into thyrocyte progenitors that can form functional follicles if further cultured in Matrigel (Antonica et al., 2012; Ma et al., 2015). These two convergent in vitro studies emphasize the essential role of basement membrane and extracellular matrix proteins for the development of a 3D, cyst-like or follicular structure.

In vivo, we observed reduced expression of laminin α1 and collagen type IV in Smad1/5[dKO]. Few reports have suggested a direct role for BMP signaling in basement membrane synthesis and deposition. During ductus arteriosus closure, Bmp9 and Bmp10 are required to stimulate endothelial cell differentiation and extracellular matrix deposition (Levet et al., 2015). In kidney mesangial cells, Smad1 directly controls the expression of collagen type IV α1 and α2, which leads to glomerular basement membrane thickening (Abe et al., 2004; Matsubara et al., 2015). Thus, cumulative evidence indicates that BMP-Smad signaling can regulate tissue morphogenesis by controlling the expression and/ or deposition of extracellular matrix proteins.

Analysis of basement membrane proteins in Vegfa[KO] also revealed decreased type IV collagen signal (Fig. 5A), most probably owing to the absence of endothelial cells (Hick et al., 2013). In addition, we found impaired epithelial laminin α1 assembly in Vegfa[KO] (data not shown). This suggests that endothelial cell invasion into the epithelial mass, by disrupting multidirectional epithelial cell-cell contacts and inducing interstitial matrix deposition that individualizes cell cords then microfollicles, would indirectly stimulate epithelial basement membrane assembly, as in MDCK cells grown in Matrigel.

Laminin deposition is the primary event of basement membrane formation, and induces the secondary assembly of the type IV collagen meshwork (Morrissey and Sherwood, 2015; Pöschl et al., 2004). In turn, the collagen IV meshwork is essential for integrity, stability and functionality of the basement membrane (Pöschl et al., 2004; Yurchenco, 2011). We thus propose that the addition of exogenous, eEPC-derived laminin-111 was sufficient to stimulate the organization of epithelial cells in follicles in control thyroid lobes, and to rescue follicle formation defects in Smad1/5[dKO] and Vegfa[KO], by promoting the assembly of endogenous laminin and type IV collagen scaffolds. Rescue of folliculogenesis in Smad1/5[dKO] and Vegfa[KO] thus indicates that basement membrane assembly is a critical step in folliculogenesis, downstream of epithelial BMP signaling and of endothelial cell invasion.

In conclusion, we propose a model that places epithelial basement membrane assembly in the developing thyroid gland as a crucial signal to orient epithelial cell polarization and promote their organization into follicles. First, epithelial cells from the thyroid

DEVELOPMENT

primordium produce Vegfa; at this step, epithelial BMP-Smad signaling participates in *Vegfa* gene expression. Second, upon Vegfa-dependent endothelial cell recruitment and invasion into the thyroid epithelial cell mass, multidirectional epithelial cell-cell contacts are disrupted while lateral contacts are preserved. This triggers, together with continued BMP-Smad signaling, epithelial cell production and deposition of their own basement membrane proteins. Finally, epithelial basement membrane assembly orients the epithelial cells, promotes the apical delivery of ezrin$^+$ vesicles and the individualization of follicles.

MATERIALS AND METHODS
Animals
Smad1/5 floxed, *Vegfa* floxed, Pax8-Cre and BRE-GFP mice were obtained from A. Zwijsen and E. J. Robertson (Arnold et al., 2006; Umans et al., 2003), N. Ferrara (Genentech) (Gerber et al., 1999), M. Busslinger (Bouchard et al., 2004) and S.C.d.S.L. (Monteiro et al., 2008), respectively. All other mice were of the CD1 strain. Mice were raised and treated according to the guidelines of laboratory animal care of the University Animal Welfare Committee, Université Catholique de Louvain.

Dissection and culture of thyroid explants
Thyroid lobes were microdissected from E14.5 mouse embryos and processed as described (Delmarcelle et al., 2014). DMH1 (Sigma-Aldrich) was dissolved in DMSO and used at 3 or 10 µM. Recombinant mouse Bmp4 (R&D Systems) was reconstituted at 100 µg/ml in 4 mM HCl containing 0.1% BSA and added at 20 ng/ml to the culture medium. Control explants were exposed to the same concentration of vehicle as the test samples. Thyroid lobes were maintained in culture for 3 or 4 days, and processed for RNA extraction and immunolabeling as described (Delmarcelle et al., 2014).

Histology, immunolabeling and morphometric analyses
Thyroids were microdissected and fixed for 1 h with 4% formaldehyde in PBS and processed for paraffin embedding. Sections (8 µm) were stained with Hematoxylin and Eosin (H&E). Immunofluorescence on thyroid gland sections from embryos or explants was performed as described previously (Pierreux et al., 2006). Antibodies and dilutions are shown in Table S2. Nuclei were counterstained with Hoechst (Sigma) in PBS during incubation with secondary antibody. For immunoperoxidase, the Envision system (Dako) was used. Whole histological sections were recorded with Mirax Scan (Zeiss). Fluorescence on sections was observed with a Zeiss Cell Axiovert 200 inverted fluorescence microscope or with a Zeiss Cell Observer spinning disk (COSD) microscope. For quantification of follicles, at least 18 sections in four independent explants were counted. Endothelial and epithelial surface was quantified using Axiovision 4.8.2 software (Zeiss). Briefly, images were prepared as a binary mask, filled and the surface area was calculated on six images/section spanning 360 µm of three controls and three *Smad1/5*^{dKO} thyroids. The epithelial to endothelial surface ratio was then calculated.

T$_3$, T$_4$ and TSH level measurements
T$_3$ and T$_4$ concentrations were measured by coated-tube radioimmunoassay (RIA) (Siemens Medical Solution Diagnostics). Plasma TSH concentrations were measured using a sensitive, heterologous, disequilibrium double-antibody precipitation RIA as described previously (Pohlenz et al., 1999). Hormone levels were measured in 16 female and 15 male mice.

RNA extraction and real-time RT-PCR
Total RNA was extracted from microdissected thyroid lobes, cultured explants or FRTL-5 cells using Trizol reagent (Thermo Scientific) and phenol/chloroform extraction (Delmarcelle et al., 2014). RNA (0.5-1 µg) was reverse transcribed with random hexamers using Moloney murine leukemia virus reverse transcriptase (Invitrogen). Real-time quantitative PCR was performed using the KAPA SYBR Fast qPCR Kit (Sopachem). Primer sequences are described in Table S3. *Actb* and *Rpl27* were used as

reference genes and relative changes in the target gene to reference gene mRNA ratio were determined by transformation of threshold cycles to absolute mRNA numbers (Dupasquier et al., 2014) or using the ΔΔCt method.

Embryonic endothelial progenitor cell-conditioned medium (eEPC-CM)
Previously established mouse eEPCs (Hatzopoulos et al., 1998; Kupatt et al., 2005) were used for no more than 6 months after being thawed, as described (Sbaa et al., 2006). The preparation of CM was adapted from Hick et al. (2013). Briefly, 90% confluent cells were incubated for 24 h in M199 medium (Thermo Scientific) without serum (6 ml for a 7.8 cm^2 dish). Supernatant was first centrifuged at 1900 *g* for 5 min to remove floating cells or large debris, then at 17,000 *g* for 20 min and finally concentrated 10× by centrifugation at 1900 *g* for 5 min in Amicon Ultra 50 K units. The 10× concentrated medium was supplemented with 10% FCS before use. Mass spectrometry was performed as described (Cho et al., 2014).

Cell culture
Fisher rat thyroid follicular FRTL-5 cells (Sigma) were cultured in Coon's modified F12 medium as previously described (Craps et al., 2015) and were used within 6 months of purchase. Cells were grown in 12-well tissue culture dishes for 24 h before treatment with BMP ligands. Recombinant mouse Bmp2, 4, 5 and 7 (R&D Systems) were reconstituted in 4 mM HCl containing 0.1% BSA at 100-150 µg/ml and used as a mix of 25 ng/ml (Bmp2), 5 ng/ml (Bmp4), 150 ng/ml (Bmp5) and 75 ng/ml (Bmp7). After 8 h, cells were lysed in Trizol reagent and RNA was extracted.

Lentiviral infection
Lentiviral constructs driving expression of shRNA against laminin α1 were generated as described previously (Gerin et al., 2010). Briefly, the pGIPZ lentiviral vectors containing a shRNA against laminin α1, α5, β1 and γ1 or the pGIPZ empty vector (Open Biosystems) were transfected into HEK293T cells for lentiviral production. Packaging was performed using a second-generation plasmid system (psPAX2 and pMD2.G; Addgene plasmids 12,259 and 12,260, respectively) by transient transfection using the calcium phosphate co-precipitation method. We used 8.4 µg lentiviral vectors, 8.4 µg psPAX2 and 4.2 µg pMD2.G per 6-cm tissue culture dish. After 24 h of transfection, eEPCs were infected with filtrated lentiviral particles and 4 mg/ml Polybrene (Sigma). Infected cells were selected for 4 days with 2 µg/ml puromycin (Merck). CM was prepared as above.

Western blotting
Western blotting was performed as described (Cominelli et al., 2014). Briefly, cells were lysed in RIPA buffer and protein concentration was measured by bicinchoninic acid assay. Then, 30 µg cell protein extract or a corresponding volume of 10×CM was loaded with 2% SDS and 10 mM DTT sample buffer on 5% polyacrylamide gels (4% stacking gel), resolved by SDS-PAGE and transferred onto PVDF membrane (Polyscreen PVDF transfer membrane, PerkinElmer). Blots were blocked and incubated overnight at 4°C with primary antibody: rabbit anti-laminin α1 (1/1000; Sasaki et al., 2002); mouse anti-ezrin (1/1000; Thermo Scientific; Table S2). After washes and incubation with the appropriate secondary antibody, immunoreactive bands were visualized by chemiluminescence (Supersignal West Femto maximum sensitivity substrate mixed with Supersignal West Pico chemiluminescent substrate, Thermo Scientific) and acquired using a 4000MM Image Station (Eastman Kodak). For silver staining, gels are stained using the Silverquest Staining Kit (Invitrogen).

Electron microscopy
Control and *Smad1/5*^{dKO} thyroid lobes were rinsed with 155 mM NaCl, fixed by 2% (v/v) glutaraldehyde in 0.1 M sodium cacodylate buffer pH 7.4 for 30 min at 4°C, and washed three times with 50 mM Tris-HCl pH 6.0 for 10 min. Cells were post-fixed with 1% (w/v) OsO$_4$/2% KFe(CN)$_6$ solution (reduced osmium) and stained en bloc with 1% uranyl acetate for 2 h and pelleted in 2% agar. Pellets were dehydrated in a graded ethanol series and embedded in Spurr resin. Ultrathin (70 nm nominal) sections were obtained

DEVELOPMENT

with a Reichert ultramicrotome, collected on copper/rhodium 400 mesh Maxtaform grids (EMS, UK) and contrasted with 3% uranyl acetate followed by lead citrate, each for 10 min. Grids were washed with water, dried, and analyzed in an FEI CM12 electron microscope operating at 80 kV.

Statistics

Data are presented as mean±s.e.m. Quantification was performed on multiple sections from at least three thyroid lobes for each genotype. Mann–Whitney U-test and one-way ANOVA followed by Bonferroni's multiple comparison tests were performed using Prism software (GraphPad).

References

Abe, H., Matsubara, T., Iehara, N., Nagai, K., Takahashi, T., Arai, H., Kita, T. and Doi, T. (2004). Type IV collagen is transcriptionally regulated by Smad1 under advanced glycation end product (AGE) stimulation. J. Biol. Chem. 279, 14201-14206.

Andrew, D. J. and Ewald, A. J. (2010). Morphogenesis of epithelial tubes: Insights into tube formation, elongation, and elaboration. Dev. Biol. 341, 34-55.

Antonica, F., Kasprzyk, D. F., Opitz, R., Iacovino, M., Liao, X.-H., Dumitrescu, A. M., Refetoff, S., Peremans, K., Manto, M., Kyba, M. et al. (2012). Generation of functional thyroid from embryonic stem cells. Nature 491, 66-71.

Arnold, S. J., Maretto, S., Islam, A., Bikoff, E. K. and Robertson, E. J. (2006). Dose-dependent Smad1, Smad5 and Smad8 signaling in the early mouse embryo. Dev. Biol. 296, 104-118.

Bai, Y., Wang, J., Morikawa, Y., Bonilla-Claudio, M., Klysik, E. and Martin, J. F. (2013). Bmp signaling represses Vegfa to promote outflow tract cushion development. Development 140, 3395-3402.

Bouchard, M., Souabni, A. and Busslinger, M. (2004). Tissue-specific expression of cre recombinase from the Pax8 locus. Genesis 38, 105-109.

Bryant, D. M., Datta, A., Rodríguez-Fraticelli, A. E., Peränen, J., Martín-Belmonte, F. and Mostov, K. E. (2010). A molecular network for de novo generation of the apical surface and lumen. Nat. Cell Biol. 12, 1035-1045.

Cho, S.-H., Szewczyk, J., Pesavento, C., Zietek, M., Banzhaf, M., Roszczenko, P., Asmar, A., Laloux, G., Hov, A.-K., Leverrier, P. et al. (2014). Detecting envelope stress by monitoring beta-barrel assembly. Cell 159, 1652-1664.

Colin, I. M., Denef, J.-F., Lengelé, B., Many, M.-C. and Gérard, A.-C. (2013). Recent insights into the cell biology of thyroid angiofollicular units. Endocrinol. Rev. 34, 209-238.

Cominelli, A., Gaide Chevronnay, H. P., Lemoine, P., Courtoy, P. J., Marbaix, E. and Henriet, P. (2014). Matrix metalloproteinase-27 is expressed in CD163 +/CD206+ M2 macrophages in the cycling human endometrium and in superficial endometriotic lesions. Mol. Hum. Reprod. 20, 767-775.

Craps, J., Wilvers, C., Joris, V., De Jongh, B., Vanderstraeten, J., Lobysheva, I., Balligand, J.-L., Sonveaux, P., Gilon, P., Many, M.-C. et al. (2015). Involvement

of nitric oxide in iodine deficiency-induced microvascular remodeling in the thyroid gland: role of nitric oxide synthase 3 and ryanodine receptors. Endocrinology 156, 707-720.

De Felice, M. and Di Lauro, R. (2004). Thyroid development and its disorders: genetics and molecular mechanisms. Endocrinol. Rev. 25, 722-746.

Deckers, M. M. L., van Bezooijen, R. L., van der Horst, G., Hoogendam, J., van der Bent, C., Papapoulos, S. E. and Löwik, C. W. G. M. (2002). Bone morphogenetic proteins stimulate angiogenesis through osteoblast-derived vascular endothelial growth factor A. Endocrinology 143, 1545-1553.

Delmarcelle, A. S., Villacorte, M., Hick, A. C. and Pierreux, C. E. (2014). An ex vivo culture system to study thyroid development. J. Vis. Exp. 88, e51641.

Dupasquier, S., Delmarcelle, A.-S., Marbaix, E., Cosyns, J.-P., Courtoy, P. J. and Pierreux, C. E. (2014). Validation of housekeeping gene and impact on normalized gene expression in clear cell renal cell carcinoma: critical reassessment of YBX3/ZONAB/CSDA expression. BMC Mol. Biol. 15, 9.

Eom, D. S., Amarnath, S., Fogel, J. L. and Agarwala, S. (2011). Bone morphogenetic proteins regulate neural tube closure by interacting with the apicobasal polarity pathway. Development 138, 3179-3188.

Fagman, H. and Nilsson, M. (2010). Morphogenesis of the thyroid gland. Mol. Cell. Endocrinol. 323, 35-54.

Fagman, H., Andersson, L. and Nilsson, M. (2006). The developing mouse thyroid: embryonic vessel contacts and parenchymal growth pattern during specification, budding, migration, and lobulation. Dev. Dyn. 235, 444-455.

Gerber, H. P., Hillan, K. J., Ryan, A. M., Kowalski, J., Keller, G. A., Rangell, L., Wright, B. D., Radtke, F., Aguet, M. and Ferrara, N. (1999). VEGF is required for growth and survival in neonatal mice. Development 126, 1149-1159.

Gerin, I., Clerbaux, L.-A., Haumont, O., Lanthier, N., Das, A. K., Burant, C. F., Leclercq, I. A., MacDougald, O. A. and Bommer, G. T. (2010). Expression of miR-33 from an SREBP2 intron inhibits cholesterol export and fatty acid oxidation. J. Biol. Chem. 285, 33652-33661.

Green, M. D., Chen, A., Nostro, M.-C., d'Souza, S. L., Schaniel, C., Lemischka, I. R., Gouon-Evans, V., Keller, G. and Snoeck, H.-W. (2011). Generation of anterior foregut endoderm from human embryonic and induced pluripotent stem cells. Nat. Biotechnol. 29, 267-272.

Hao, J., Ho, J. N., Lewis, J. A., Karim, K. A., Daniels, R. N., Gentry, P. R., Hopkins, C. R., Lindsley, C. W. and Hong, C. C. (2010). In vivo structure-activity relationship study of dorsomorphin analogues identifies selective VEGF and BMP inhibitors. ACS Chem. Biol. 5, 245-253.

Hatzopoulos, A. K., Folkman, J., Vasile, E., Eiselen, G. K. and Rosenberg, R. D. (1998). Isolation and characterization of endothelial progenitor cells from mouse embryos. Development 125, 1457-1468.

He, C. and Chen, X. (2005). Transcription regulation of the vegf gene by the BMP/ Smad pathway in the angioblast of zebrafish embryos. Biochem. Biophys. Res. Commun. 329, 324-330.

Hick, A.-C., Delmarcelle, A.-S., Bouquet, M., Klotz, S., Copetti, T., Forez, C., Van Der Smissen, P., Sonveaux, P., Collet, J.-F., Feron, O. et al. (2013). Reciprocal epithelial:endothelial paracrine interactions during thyroid development govern follicular organization and C-cells differentiation. Dev. Biol. 381, 227-240.

Kupatt, C., Horstkotte, J., Vlastos, G. A., Pfosser, A., Lebherz, C., Semisch, M., Thalgott, M., Büttner, K., Browarzyk, C., Mages, J. et al. (2005). Embryonic endothelial progenitor cells expressing a broad range of proangiogenic and remodeling factors enhance vascularization and tissue recovery in acute and chronic ischemia. FASEB J. 19, 1576-1578.

Kurmann, A. A., Serra, M., Hawkins, F., Rankin, S. A., Mori, M., Astapova, I., Ullas, S., Lin, S., Bilodeau, M., Rossant, J. et al. (2015). Regeneration of thyroid function by transplantation of differentiated pluripotent stem cells. Cell Stem Cell 17, 527-542.

Lammert, E., Cleaver, O. and Melton, D. (2001). Induction of pancreatic differentiation by signals from blood vessels. Science 294, 564-567.

Lazarus, A., Del-Moral, P. M., Ilovich, O., Mishani, E., Warburton, D. and Keshet, E. (2011). A perfusion-independent role of blood vessels in determining branching stereotypy of lung airways. Development 138, 2359-2368.

Levet, S., Ouarné, M., Ciais, D., Coutton, C., Subileau, M., Mallet, C., Ricard, N., Bidart, M., Debillon, T., Faravelli, F. et al. (2015). BMP9 and BMP10 are necessary for proper closure of the ductus arteriosus. Proc. Natl. Acad. Sci. USA 112, E3207-E3215.

Longmire, T. A., Ikonomou, L., Hawkins, F., Christodoulou, C., Cao, Y., Jean, J. C., Kwok, L. W., Mou, H., Rajagopal, J., Shen, S. S. et al. (2012). Efficient derivation of purified lung and thyroid progenitors from embryonic stem cells. Cell Stem Cell 10, 398-411.

Ma, R., Latif, R. and Davies, T. F. (2015). Human embryonic stem cells form functional thyroid follicles. Thyroid 25, 455-461.

Macias, M. J., Martin-Malpartida, P. and Massagué, J. (2015). Structural determinants of Smad function in TGF-beta signaling. Trends Biochem. Sci. 40, 296-308.

Matsubara, T., Araki, M., Abe, H., Ueda, O., Jishage, K.-i., Mima, A., Goto, C., Tominaga, T., Kinosaki, M., Kishi, S. et al. (2015). Bone morphogenetic protein 4 and Smad1 mediate extracellular matrix production in the development of diabetic nephropathy. Diabetes 64, 2978-2990.

Monteiro, R. M., de Sousa Lopes, S. M. C., Bialecka, M., de Boer, S., Zwijsen, A. and Mummery, C. L. (2008). Real time monitoring of BMP Smads transcriptional activity during mouse development. *Genesis* **46**, 335-346.

Morrissey, M. A. and Sherwood, D. R. (2015). An active role for basement membrane assembly and modification in tissue sculpting. *J. Cell Sci.* **128**, 1661-1668.

Nilsson, M. and Fagman, H. (2013). Mechanisms of thyroid development and dysgenesis: an analysis based on developmental stages and concurrent embryonic anatomy. *Curr. Top. Dev. Biol.* **106**, 123-170.

Petryk, A., Anderson, R. M., Jarcho, M. P., Leaf, I., Carlson, C. S., Klingensmith, J., Shawlot, W. and O'Connor, M. B. (2004). The mammalian twisted gastrulation gene functions in foregut and craniofacial development. *Dev. Biol.* **267**, 374-386.

Pierreux, C. E., Poll, A. V., Kemp, C. R., Clotman, F., Maestro, M. A., Cordi, S., Ferrer, J., Leyns, L., Rousseau, G. G. and Lemaigre, F. P. (2006). The transcription factor hepatocyte nuclear factor-6 controls the development of pancreatic ducts in the mouse. *Gastroenterology* **130**, 532-541.

Pierreux, C. E., Cordi, S., Hick, A. C., Achouri, Y., Ruiz de Almodovar, C., Prévot, P. P., Courtoy, P. J., Carmeliet, P. and Lemaigre, F. P. (2010). Epithelial: endothelial cross-talk regulates exocrine differentiation in developing pancreas. *Dev. Biol.* **347**, 216-227.

Pohlenz, J., Maqueem, A., Cua, K., Weiss, R. E., Van Sande, J. and Refetoff, S. (1999). Improved radioimmunoassay for measurement of mouse thyrotropin in serum: strain differences in thyrotropin concentration and thyrotroph sensitivity to thyroid hormone. *Thyroid* **9**, 1265-1271.

Pöschl, E., Schlötzer-Schrehardt, U., Brachvogel, B., Saito, K., Ninomiya, Y. and Mayer, U. (2004). Collagen IV is essential for basement membrane stability but dispensable for initiation of its assembly during early development. *Development* **131**, 1619-1628.

Ramasamy, S. K., Kusumbe, A. P. and Adams, R. H. (2015). Regulation of tissue morphogenesis by endothelial cell-derived signals. *Trends Cell Biol.* **25**, 148-157.

Sasaki, T., Giltay, R., Talts, U., Timpl, R. and Talts, J. F. (2002). Expression and distribution of laminin alpha1 and alpha2 chains in embryonic and adult mouse tissues: an immunochemical approach. *Exp. Cell Res.* **275**, 185-199.

Sbaa, E., DeWever, J., Martinive, P., Bouzin, C., Frérart, F., Balligand, J.-L., Dessy, C. and Feron, O. (2006). Caveolin plays a central role in endothelial progenitor cell mobilization and homing in SDF-1-driven postischemic vasculogenesis. *Circ. Res.* **98**, 1219-1227.

Shao, E. S., Lin, L., Yao, Y. and Bostrom, K. I. (2009). Expression of vascular endothelial growth factor is coordinately regulated by the activin-like kinase receptors 1 and 5 in endothelial cells. *Blood* **114**, 2197-2206.

Shimizu, T., Magata, F., Abe, Y. and Miyamoto, A. (2012). Bone morphogenetic protein 4 (BMP-4) and BMP-7 induce vascular endothelial growth factor expression in bovine granulosa cells. *Anim. Sci. J.* **83**, 663-667.

Umans, L., Vermeire, L., Francis, A., Chang, H., Huylebroeck, D. and Zwijsen, A. (2003). Generation of a floxed allele of Smad5 for cre-mediated conditional knockout in the mouse. *Genesis* **37**, 5-11.

Wang, A. Z., Ojakian, G. K. and Nelson, W. J. (1990a). Steps in the morphogenesis of a polarized epithelium. I. Uncoupling the roles of cell-cell and cell-substratum contact in establishing plasma membrane polarity in multicellular epithelial (MDCK) cysts. *J. Cell Sci.* **95**, 137-151.

Wang, A. Z., Ojakian, G. K. and Nelson, W. J. (1990b). Steps in the morphogenesis of a polarized epithelium. II. Disassembly and assembly of plasma membrane domains during reversal of epithelial cell polarity in multicellular epithelial (MDCK) cysts. *J. Cell Sci.* **95**, 153-165.

Yurchenco, P. D. (2011). Basement membranes: cell scaffoldings and signaling platforms. *Cold Spring Harb. Perspect. Biol.* **3**, a004911.

DEVELOPMENT
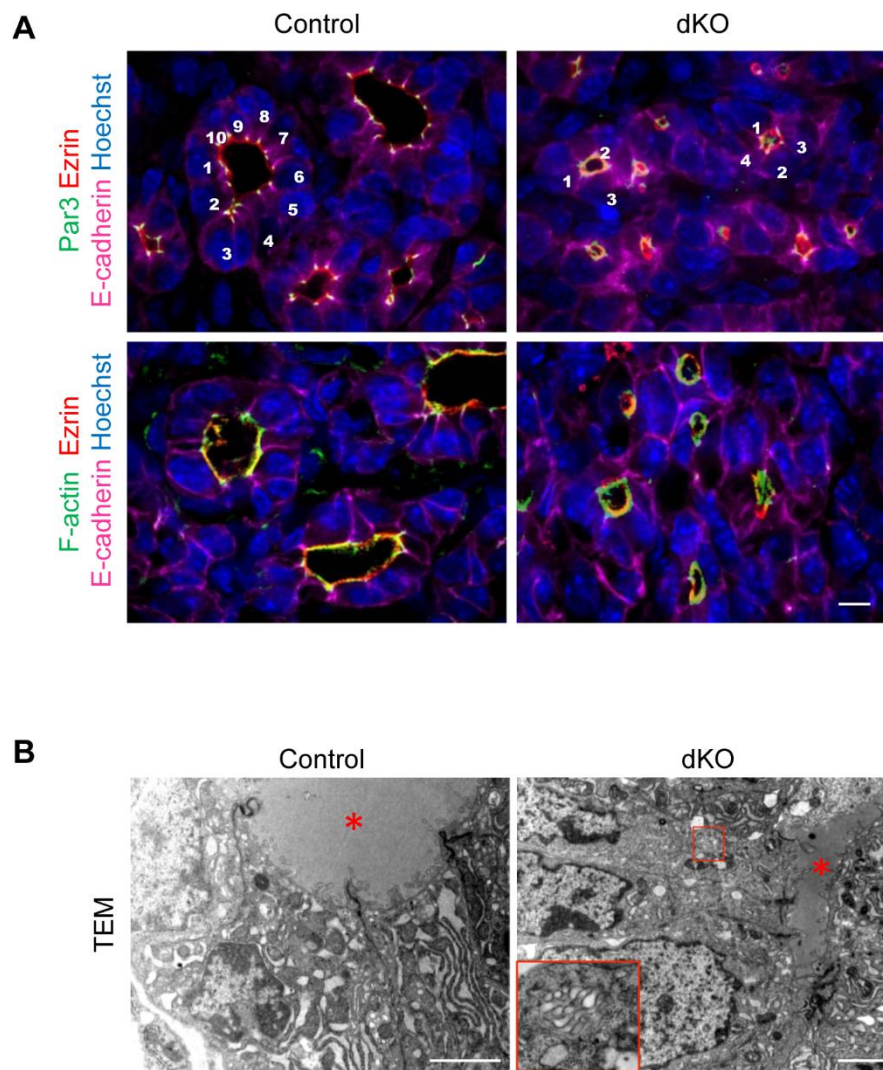
Figure S1. Apical polarity is not affected in Smad1/5[dKO] at E18.5. **(A)** Apical polarity marker, Par3 and cytoplasmic stratification marker, F-actin, show no difference in signal intensity and localization between Smad1/5[dKO] and control. Numbers illustrate counting of cells facing lumina (see Fig. 3D) **(B)** Transmission electron microscopy of control thyroid reveals cuboidal epithelial cells surrounding a large lumen filled with homogeneous colloid (*), in which tight junctions and apical microvilli are projecting. In Smad1/5[dKO], columnar thyrocytes also display tight junctions and apical microvilli projecting in non-expanded and smaller lumen (*). Inset illustrates microvilli inclusion body at a distance from apical lumen. Bar, (A) 10 μm and (B) 2 μm.
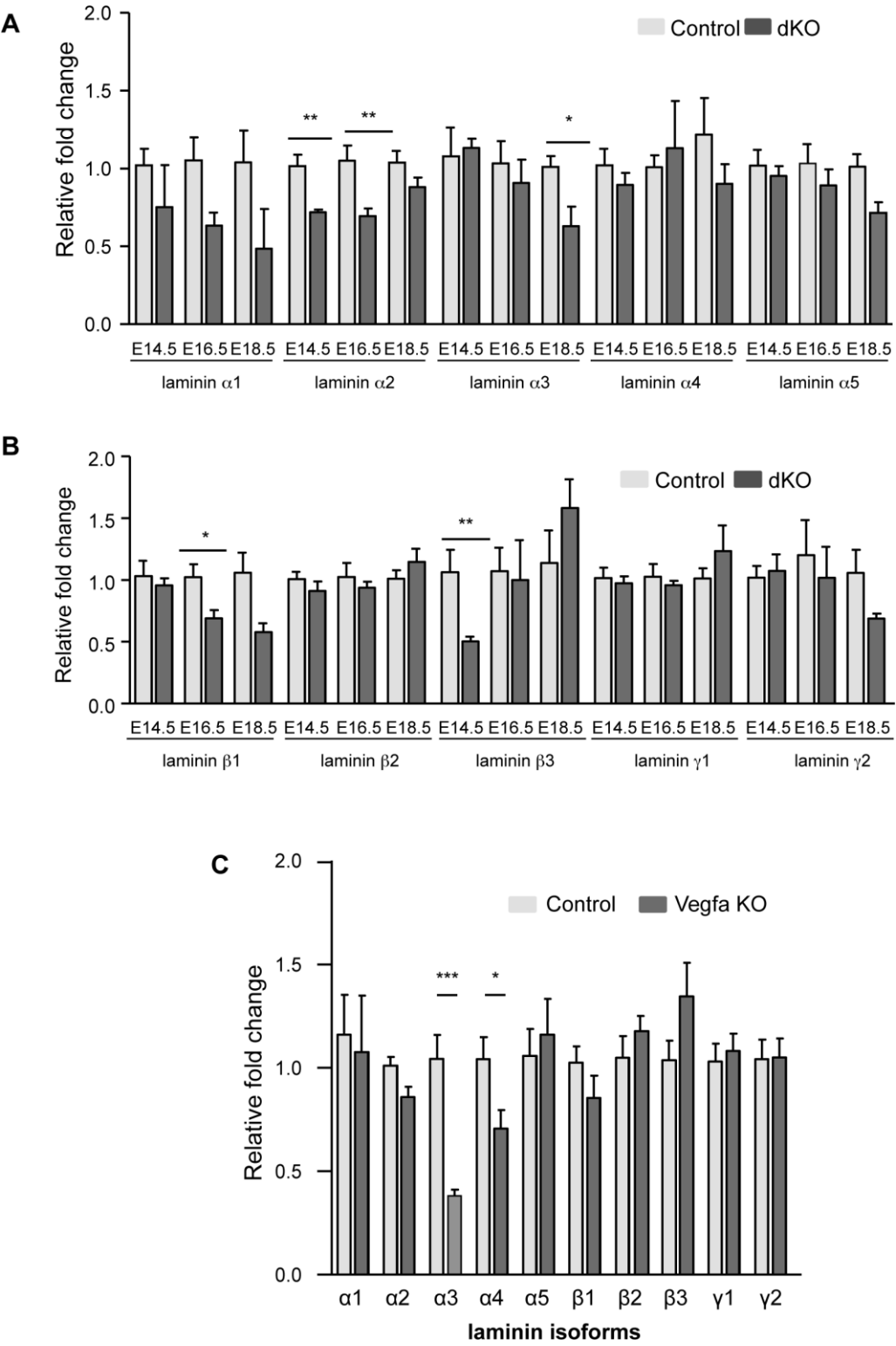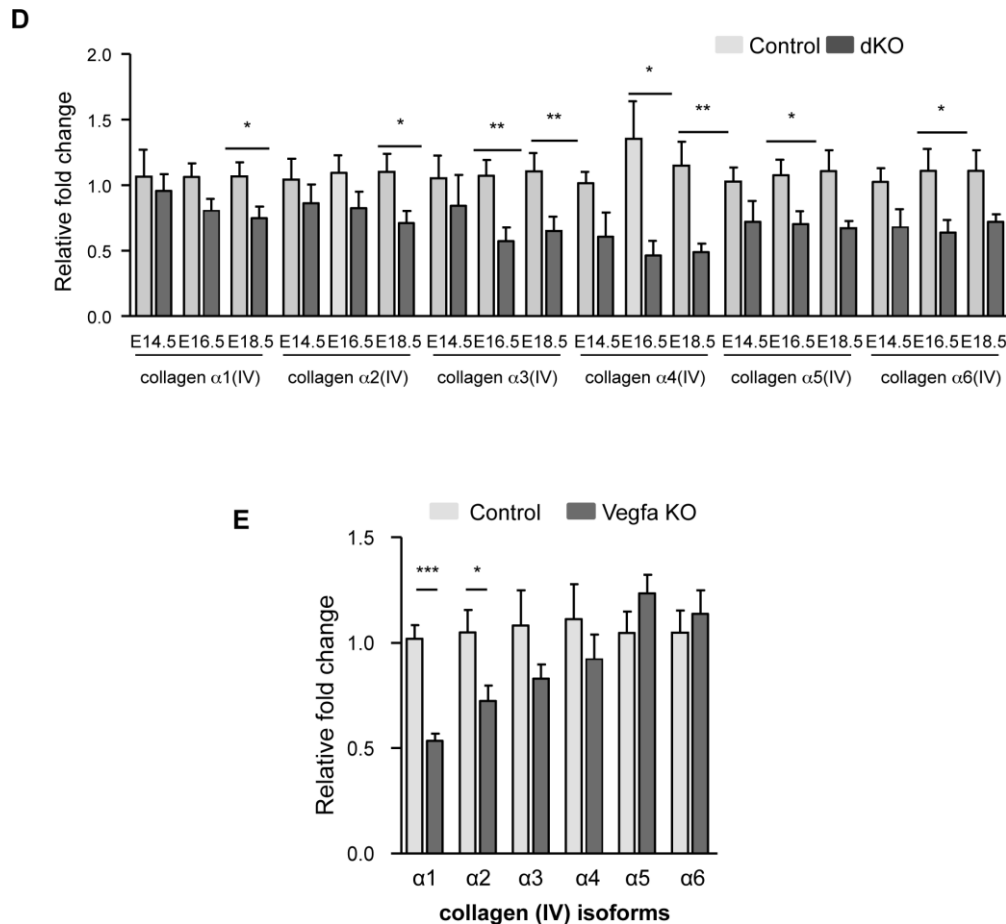
Figure S2. Expression of *laminin* α, β and γ chains in Smad1/5[dKO] and Vegfa[KO] mice. (A) Quantification of *laminin* $\alpha$ in control and Smad1/5[dKO] from E14.5 to E18.5. Expression of *laminin* $\alpha 1$ shows a trend to a decrease from E14.5 to E18.5. Variability may come from remaining parathyroid cells, highly expressing this laminin isoform. *Laminin* $\alpha 2$ expression was significantly reduced at E14.5 and E16.5 but was normal at E18.5. *Laminin* $\alpha 3$ was significantly reduced at E18.5. Expression levels of *laminin* $\alpha 4$ and $\alpha 5$ were statistically not different from E14.5 to E18.5. **(B)** Quantification of *laminin* β *and* γ in control and Smad1/5[dKO] from E14.5 to E18.5. Expression of *laminin* $\beta 1$ was reduced from E16.5. Expression of *laminin* $\beta 3$ showed 50% reduction at E14.5 and no change at E18.5. *Laminin* $\beta 2$, $\gamma 1$ and $\gamma 2$ expression were comparable to control. **(C)** Quantification of *laminins* in Vegfa[KO] at P0. *Laminin* $\alpha 3$ and $\alpha 4$ were significantly reduced as compared to control. All the other *laminins* were normally expressed. **(D)** Quantification of *collagen IV* genes in Smad1/5[dKO] from E14.5 to E18.5. Expression of *collagen IV* $\alpha 1$ and *IV* $\alpha 2$, showed no change at E14.5 and E16.5 but their expression levels were significantly reduced at E18.5. *Collagen IV* $\alpha 3$ and *IV* $\alpha 4$ showed no difference at E14.5 but significantly reduced at E16.5 and E18.5. *Collagen IV* $\alpha 5$ and *IV* $\alpha 6$ were reduced from E14.5 onwards, but only statistically at E16.5. **(E)** Quantification of *collagen IV* genes in Vegfa[KO] at P0. *collagen IV a1*, *a2* were significantly reduced as compared to control. All the other *collagen IV* genes were normally expressed. All mRNAs were normalized to either *RPL27* or *β-actin* *p<0.05; ** p<0.001; *** p<0.0001 using Mann Whitney U test (n≥3). Data are presented as means ± S.E.M.
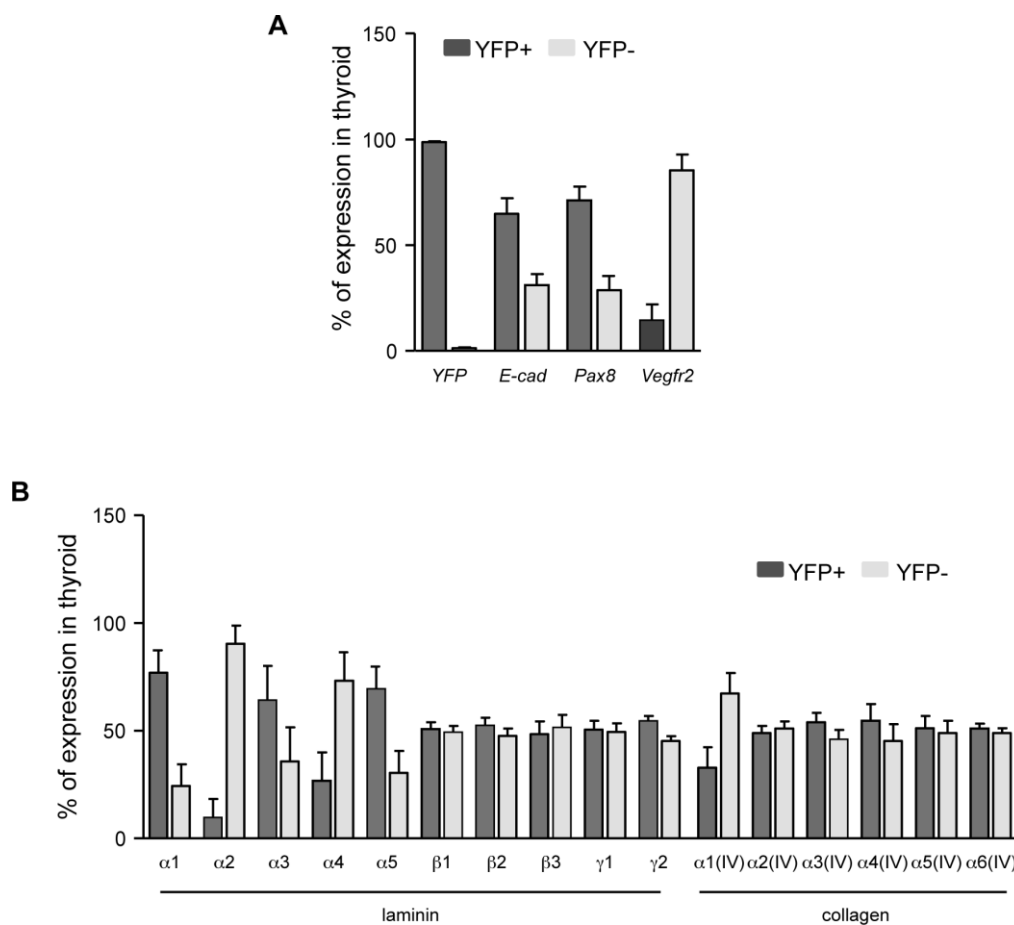
Figure S3. Expression of *laminin* and *collagen* in FACS-sorted Pax8/CRE⁺ cells. (A)
Percent of expression of selected genes in YFP⁺ and YFP⁻ populations reveals enrichment of
YFP, *E-cadherin* and *Pax8* in YFP⁺ (i.e. thyrocytes progenitors) population and absence of
Vegfr2 in this population. (B) Percent of expression of *laminin* α, β, and γ and *collagen type
IV* in YFP⁺ and YFP⁻ populations reveals enrichment of *laminin* $\alpha1$ and $\alpha5$ in YFP⁺
population and enrichment of *laminin* $\alpha2$, $\alpha4$ and *collagen* $\alpha1(IV)$ in YFP⁻ population. All
mRNAs were normalized to *β-actin*. Data are presented as means ± S.E.M. (n=4).
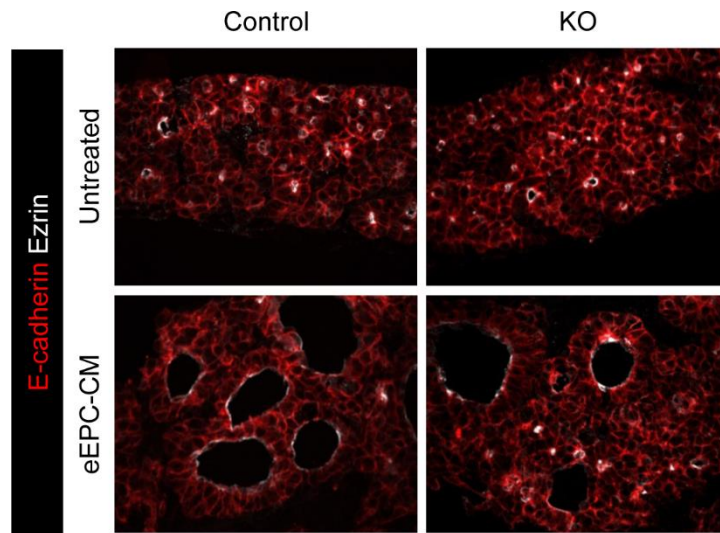
Figure S4. **eEPC-CM rescues follicle formation defect in Vegfa^{KO} thyroid glands.**
Treatment of E14.5 thyroid glands of control and Vegfa^{KO} mice with eEPC-CM during 3
days, stimulates follicle formation and lumen size enlargement, as visualized by ezrin (white)
and E-cadherin (red) labeling. Bar, 20 μm.

Table S1. Candidate folliculogenic factors found by mass spectrometry analysis of eEPC-CM

Accession	Name	Score	MW (kDa)
Q5NCU4	SPARC	71.04	34.3
P07724	Serum albumin	67.97	68.6
F8VQJ3	Laminin subunit gamma 1	60.83	177.1
P06151	L-lactate dehydrogenase A chain	53.01	36.5
P09103	Protein disulfide-isomerase	50.57	57.0
P02469	Laminin subunit beta 1	48.94	197.0
P08113	Endoplasmin	40.42	92.4
G3x9D5	Histone H2B	35.83	13.4
P14211	Calreticulin	35.32	48.0
F8VQ40	Laminin subunit alpha-1	34.57	337.9
P60710	Actin, cytoplasmic1	31.37	41.7
P68033	Actin, alpha cardiac muscle	25.63	42.0
Q01768	Nucleoside diphosphate kinase B	23.24	17.4
P20029	78 kDa glucose-regulated protein	21.38	72.4
Q5SQB0	Nucleophosmin	19.06	29.5

Table S2. Primary antibodies

Primary antibody	species	dilution	Source	Catalog number
E-cadherin	mouse	1/200	BD Biosciences	610182
Pan-Laminin	rabbit	1/100	Sigma	L9393
PECAM	rat	1/100	BD Biosciences	550274
PECAM	rat	1/20	Dianova	DIA 310
Ezrin	mouse	1/300	Thermo Scientific	MS-661
Calcitonin	rabbit	1/1000	Dako	A0576
GFP	rabbit	1/200	Cell Signaling	2956S
Par3	rabbit	1/200	Merck/Millipore	07-330
Laminin α1	rabbit	1/1000	Gift from Dr. T. Sasaki	
Laminin α5	rabbit	1/1000	Gift from Dr. T. Sasaki	
Collagen IV	rabbit	1/500	Merck/Millipore	AB756P
Thyroglobulin	mouse	1/500	Dako	M0781
pSmad158	rabbit	1/100	Cell Signaling	9511S
pSmad15	rabbit	1/100	Cell Signaling	9516S
iodo-thyroglobulin	mouse	1/100	Gift from Dr. Ris-Stalpers	

Table S3. Primers

Gene	Primer sequences (5'-3')	Fragment size (bp)
E-cadherin	AGGGAGCTGTCTACCAAAGTG CCAGTCTCGTTTCTGTCTTC	146
VE-cadherin	GGATGTGGTGCCAGTAAACC ACCCCGTTGTCTGAGATGAG	173
Vegfr2	GCATGGAAGAGGATTCTGGA CGGCTCTTTCGCTTACTGTT	142
Vegfa mouse	GTACCTCCACCATGCCAAGT CTGCATGGTGATGTTGCTCT	265
Vegfa rat	GAGTATATCTTCAAGCCGTCCTGT TTTTCTGGCTTTGTTCTATCTTC	193
β-actin	TCCTGAGCGCAAGTACTCTGT CTGATCCACATCTGCTGGAAG	77
Nkx2.1	ATCTGAGCTGGGGTGCTGGG GCCCTGTCTGTACGCTGCGA	244
Pax8	TGCCTTTCCCCATGCTGCCTCCGTGTA GGTGGGTGGTGCGCTTGGCCTTGATGTAG	298
Foxe1	GGCGGCATCTACAAGTTCAT GGATCTTGAGGAAGCAGTCG	115
Hhex	TCAGAATCGCCGAGCTAAAT ACTGCGAACGATCCAAAGAG	152
Tpo	TGCCAACAGAAGCATGGGCAAC GCACAAAGTTCCCATTGTCCAC	424
Tg	TGGGACGTGAAAGGGGAATGGTGC GTGAGCTTTTGGAATGGCAGGCGA	394
Nis	AGCAGGCTTAGCTGTATCCC AGCCCCGTAGTAGAGATAGGAG	235
Tshr	CTGCGGGGCAAAGAGTGTGC AGGGGAGCTCTGTCAAGGCA	325
Calcitonin	TGGTTGTCAGCATCTTGCTC CTTAGATCTGGGGCTGTCCA	221
Smad 1	GCCTCTGGAATGCTGTGAGT GAACTGAGCCAGAAGGCTGT	137
Smad 5	GCAGAGCCATCACGAGCTAA CCAGAAGGCTGTGTTGTGGA	169
Smad 8	CACCGACCCTTCCAATAAC CTGGACAAAGATGCTGCTG	153
RPL 27	GCCCTGGTGGCTGGAATTGACC AAACTTGACCTTGGCCTCCCGC	233
ID2	CATCCTGTCCTTGCAGGCAT CCATTCAACGTGTTCTCCTGG	199
PECAM	ATAGGCATCAGCTGCCAGTC TCCGCTCTGCACTGGTATTC	157
Pcdh12	TGCCCCTCACCACCAATTAC GTGCTGCCCCAACAACATTT	171
Tie 1	CAGGGACCTTGACCTTGACC ATCATGGCCCGGATCACTTG	135

Esm 1	ACCTTCGGGATGGAATGCAA AGAGGTCCTGCTGGGAGATT	125
YFP	CCTCGTGACCACCTTCGG CTCAGGTAGTGGTTGTCGG	400
BMP 2	CAGCGCAATCTCCATGTTG GGGAAATATTAAAGTGTCAGCTGG	197
BMP 4	GGATCTTTACCGGCTCCAG CCAGATGTTCTTCGTGATGG	130
BMP 5	TTCCACATGGAGAAGCAGTG AAGCCCAAATTGTTCTGTGG	246
BMP 7	TCCGGTTTGATCTTTCCAAG TGGCTGTGATGTCAAACACC	224
Laminin α1	AGCTGTGTGCTTCTGGCTAC TCACTGTCACCTTCCACGAC Or CCGACAACCTCCTCTTCTACC TCTCCACTGCGAGAAAGTCA	123 or 59
Laminin α2	CTGGAGTTGGTCCTCTCAGC TGAACATCAACCTCACGGGC Or TTGCCCTCTGCCAACTGAAT TGAACATCAACCTCACGGGC	240 Or 135
Laminin α3	ATGAACAGTGAGGCAGGTGG GGACGCCTCCAATGTGTAGT	198
Laminin α4	ACGGGGAATACCTGAACGTG TCTGTGCCATCTGCCATCAC	124
Laminin α5	ACCCAAGGACCCACCTGTAG TCATGTGTGCGTAGCCTCTC	168
Laminin β1	TGGACAAGAGCAACGAGGAC TTCTGTAACTGCTGTGGCGT	147
Laminin β2	GTGTGGCTTGCATAGCCCT TCCGATGACTATTTGGGTTGTCT	121
Laminin β3	GGGAGACCATGGAAATGATG GATCTGCTCCACACGCTTCT	121
Laminin γ1	TGCCGGAGTTTGTTAATGCC CTGGTTGTTGTAGTCGGTCAG	184
Laminin γ2	GGCAGTCAGCATCAGAACAG CCCCACGTAGTGCTCAGAAG	125
Integrin α3	CCCTTCCAGACACCTCCAAC ACCACAGCTCAATCTCAGCC	230
Integrin α6	TGGACATTCTCCTGAGGGCT TGAGGGAAACACCGTCACTC	100
Integrin α7	AAGGTGGAGCCTAGCACATC TCAAAGCTGTAGAGTGGGCAG	121
Integrin β1	ATGGCCGGGGTATTTGTGAA GAAGTGGGAGCACTCCTGTG	181
Integrin β4	CAGGGAGGCTGGCTTTCAAT TTCTTGGGGTTGTCCACGAG	171
Collagen IV a1	AACAACGTCTGCAACTTCGC CTTCACAAACCGCACACCTG	135
Collagen IV a2	GGATGCCAGGGCTTAAAGGT CTGTCTCCAGGCAAACCTCC	159

Collagen IV a3	GGCCCTGAGTGGAAGGAAAG GACTCCTTGGGCTCCCTTTG	138
Collagen IV a4	GCCAGAAAGGACCAATGGGA TACTGGCCCTTTTCTGCCTG	106
Collagen IV a5	CCCCAGGACCAGATGGATTG TACTGAAGCGACGAAGGCAG	224
Collagen IV a6	GGCCTGAAAGGAGACCAAGG CTCAAATGTGCGACCAGGTG	128